The Ogooue Fan (Gabon): a modern example of deep-sea fan on a complex slope profile.

Salomé Mignard, University of Bordeaux, UMR CNRS 5805 EPOC.

Thierry Mulder, University of Bordeaux, UMR CNRS 5805 EPOC

Philippe Martinez, University of Bordeaux, UMR CNRS 5805 EPOC

Thierry Garlan, SHOM

Abstract. The effects of ~~important~~ changes in slope gradient on turbidity currents ~~velocity~~ have been investigated in different deep-sea systems both in modern and ancient environments. However, the impact of subtle gradient changes (<0.5°) on sedimentary processes along deep-sea fans still needs to be clarified. The Ogooue Fan, located in the northeastern part of the Gulf of Guinea, extends over more than 550 km westwards of the Gabonese shelf and passes through the Cameroun Volcanic Line. Here, we present the first study of acoustic data (multibeam echosounder and 3.5 kHz, very-high resolution seismic data) and piston cores covering the deep-sea part of this West African system. This study documents the architecture and sedimentary facies distribution along the fan. Detailed mapping and near-seafloor seismic dataset reveal the influence of subtle slope gradient changes (< 0.2°) along the fan morphology. The overall system corresponds to a well-developed deep-sea fan, fed by the Ogooue River ‘sedimentary load, with tributary canyons, distributary channel-levee complexes and lobes elements. However, variations in the slope gradient due to inherited salt-related structures and the presence of several seamounts, including volcanic islands, result in a more complex fan architecture and sedimentary facies distribution. In particular, turbidity currents derived from the Gabonese shelf deposit ~~a~~cross several interconnected intraslope basins located on the low gradient segments of the margin (<0.3°). The repeated spill-overs of the most energetic turbidity currents have notably led to the

incision of a large mid-system valley on a higher gradient segment of the slope (0.6°) connecting an intermediate sedimentary basin to the more distal lobe area.

Distribution and thickness of turbidite sand beds is highly variable along the system, however, turbidite sands preferentially deposit on the floor of the channel and the most proximal depositional areas. The most distal depocenters receive only the upper parts of the flows, mainly composed of fine-grained sediments. The Ogooue deep-sea fan is predominantly active during periods of low sea-level because the canyon heads are separated from terrestrial sediment sources by the broad continental shelf. However, the northern part of this system appears active during sea-level highstands. This feature is due to one deeply incised canyon, the Cape Lopez Canyon located on a narrower part of the continental shelf, which receives sediments transported by the longshore drift.

Keywords: Ogooue Fan, Gulf of Guinea, complex slope profile, turbidity currents, stepped slope

1 Introduction

Deep-sea fans are depositional sinks that host stratigraphic archives of Earth history and environmental changes (Clift and Gaedicke, 2002; Fildani and Normark, 2004; Covault et al., 2010, 2011), and are also important reservoirs of natural resources (Pettingill and Weimer, 2002). Therefore, considerable attention has been given to the problems of predicting architectures and patterns of sedimentary facies distribution in submarine fans. First models concerning the morphologies of these systems described submarine fans as cone-liked depositional areas across unconfined basin floors of low relief and gentle slope gradient (Shepard and Emery, 1941; Shepard, 1951; Dill et al., 1954; Menard, 1955; Heezen et al., 1959). However, the development of numerous studies realized on both fossil and modern fans showed that topographic complexity across the receiving basin can strongly influence the organization of architectural elements of submarines fans (Normark et al., 1983; Piper and Normark, 2009). A wide range of geometries and architectural features due to topographic obstacles has been described

in the literature. Among these features are ponded and intra-slope mini-basin due to three-dimensional confinement (Prather, 2003; Prather et al., 2012, 2017; Sylvester et al., 2015) or tortuous corridors created by topographic barriers (Smith, 2004; Hay, 2012). Spatial changes in slope gradients are also important as they cause gravity flows to accelerate or decelerate along the slope (Normark and Piper, 1991; Mulder and Alexander, 2001) allowing the construction of successive depocenters and sediment bypass areas (Smith, 2004; Deptuck, 2012; Hay, 2012). These stepped-slopes have been described along modern systems such as the Niger Delta (Jobe et al., 2017), the Gulf of Mexico (Prather et al., 1998, 2017) or offshore Angola (Hay, 2012), but also in ancient systems such as the Annot Sandstone Formation (Amy et al., 2007; Salles et al., 2014), the Karoo Basin (Spychala et al., 2015; Brooks et al., 2018) or the Lower Congo basin (Ferry et al., 2005).

On stepped-slopes where structural deformation is very slow, sediment erosion and deposition are the dominant processes that control the short-term evolution of slope. In these systems, the slope gradient variations play a key role and studies have shown that subtle gradient changes can have an important impact on flow velocity and consequently deep-sea fans organization (e.g. Kneller, 1995; Kane et al., 2010; Stevenson et al., 2013). However, despite the growing numbers of studies describing these systems, the impact of subtle changes in slope gradient on deep-sea fans organization still needs to be better apprehended.

The modern Ogooue Fan provides a new large-scale example of the influence of subtle gradient changes on deep-sea sediment routing. This system, which results from the sediment discharge of the Ogooue River, is the third largest system of the Gulf of Guinea after the Congo and the Niger fans (Séranne and Anka, 2005). However, in contrast to these two systems that have been the focus of many studies (Droz et al., 1996, 2003; Babonneau et al., 2002; Deptuck et al., 2003, 2007), the Quaternary sediments of the Gabon passive margin have been relatively poorly studied, especially in its deepest parts (Bourgoin et al., 1963; Giresse, 1969; Giresse and Odin, 1973). The regional survey of the area by the SHOM (Service Hydrographique et Océanographique de la Marine) in

85   2005 and 2010, during the OpticCongo and MOCOSED cruises, provided the first

86   extensive dataset on the Ogooue deep-sea fan, from the continental shelf to the abyssal

87   plain.

88   The objective of this paper is to document the overall fan morphology, and to link its

89   evolution with the local changes in slope gradients or topographic obstacles present in

90   the depositional area. This study contributes to the understanding of the impact of subtle

91   slope gradient changes on deep-water systems and can be used to develop predictive

92   models for systems located on stepped-slope with low to very low gradient changes

93   ($< 1°$).

94

 2 **Geological setting**
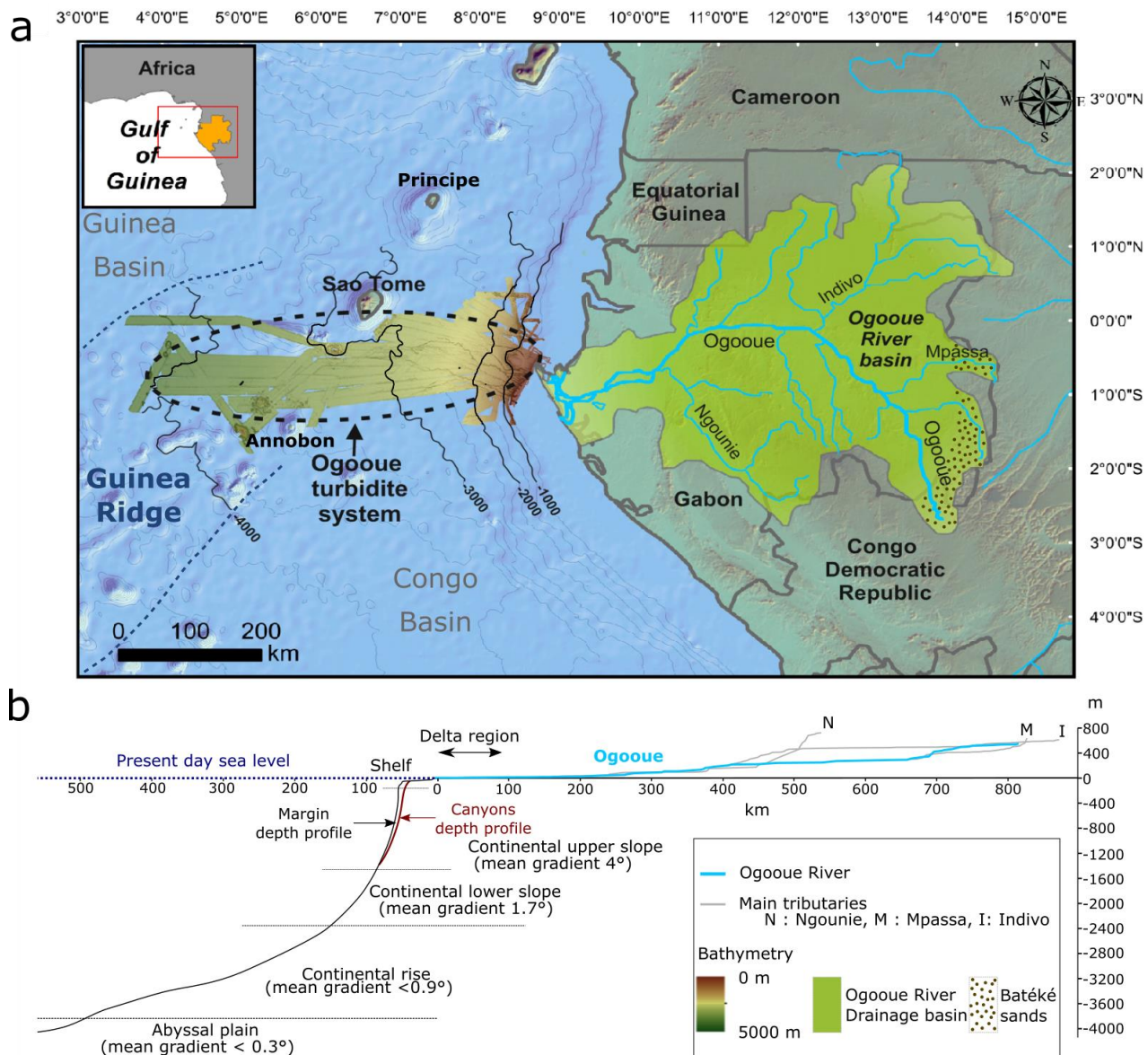
Figure 1: a) The Ogooue sedimentary system from source (river and drainage basin) to sink (Quaternary turbidite fan). b) Channel depth profile of the Ogooue River (blue) and its main tributaries (grey) and mean depth profile along the Gabonese margin.

The continental margin of the Gulf of Guinea formed during the rifting that occurred within Gondwana craton in Neocomian to lower Aptian times. Syn-rift deposits are buried by mid-late Cretaceous transgressive sediments consisting initially of evaporites, which have created salt-related deformations of the margin sediments, followed by platform carbonates (Cameron and White, 1999; Mougamba, 1999; Wonham et al., 2000; Séranne and Anka, 2005). Since the Late Cretaceous, the West African margin

has recorded clastic sedimentation fed by the denudation of the African continent (Séranne and Anka, 2005). Different periods of major uplift and canyons incision occurred from Eocene to Lower Miocene times (Rasmussen, 1996; Wonham et al., 2000; Séranne and Anka, 2005). The sediments depocenters were located basinward of the main rivers, such as the Niger, Congo, Ogooue or Orange River forming vast and thick deep-sea fans (Mougamba, 1999; Séranne and Anka, 2005; Anka et al., 2009).

The Ogooue Fan is located in the northeastern part of the Gulf of Guinea on the Gabonese continental slope. The fan develops on the Guinea Ridge, which separates the two deep Congo and Guinea basins. This region is notably characterized by the presence of several volcanic islands belonging to the Cameroon Volcanic Line (CVL) associated with rocky seamounts (Figure 1a). Geophysical studies of the volcanic line suggest that the volcanic alignment is related to a deep-mantle hot line (Déruelle et al., 2007). All the volcanoes of the CVL have been active for at least 65 Ma (Lee et al., 1994; Déruelle et al., 2007). Ar/Ar dates realized on Sao Tomé and Annobon volcanic rocks evidenced the activity of theses volcanic island over much of the Pleistocene (Lee et al., 1994; Barfod and Fitton, 2014). The MOCOSED 2010 cruise revealed that numerous mud volcanoes where associated with the toe of the slopes of the volcanic islands (Garlan et al., 2010). They form small topographic highs on the seafloor (< 20 m high and 100 m in diameter) and show active gas venting (Garlan et al., 2010).

The Quaternary Ogooue Fan extends westwards over 550 km through the CVL. Overall, the modern slope profile is concave upward, similar to that of many other passive margins. The mean slope gradient shallows from 7° on the very upper slope to < 0.3° in the abyssal plain (Figure 1b). The Gabonese continental shelf, which is relatively narrow, can be divided into two sub-parts: the south Gabon margin presenting a SE-NW orientation and the north Gabon margin presenting a SW-NE orientation. The southern part of the margin is characterized by the presence of numerous parallel straight gullies oriented perpendicular to the slope (Séranne and Nzé Abeigne, 1999; Lonergan et al., 2013). On the north Gabon margin, the area located between 1°00 S and the Mandji Island is incised by several canyons that belong to the modern Ogooue Fan (Figure 2a).

North of the Mandji Island, the seafloor reveals numerous isolated pockmarks as well as sinuous trains of pockmarks. These features are interpreted as the results of fluid migration from shallow buried channels (Gay et al., 2003; Pilcher and Argent, 2007). The Ogooue Fan is supplied by the sedimentary load of the Ogooue River, which is third largest African freshwater source in the Atlantic Ocean (Mahé et al., 1990). Despite the relatively small size of the Ogooue River basin (215,000 km²), the river mean annual discharge reaches 4,700 m^3/s due to the wet equatorial climate (Lerique et al., 1983; Mahé et al., 1990). The Ogooue River flows on a low slope gradient in a drainage basin covered essentially with thick lateritic soils that developed over the Congo craton and Proterozoic formations related to Precambrian orogenic belts (Séranne et al., 2008). The estuary area includes several lakes (Figure 1b) (Lerique et al., 1983) that contribute to the dominant muddy composition of the particle load of the Ogooue River that is estimated between 1 and 10 M t/yr. (Syvitski et al., 2005). The limited portion of sand particles in the river originates mainly from the erosion of the poorly lithified Batéké Sands located on a 550-750 m high perched plateau that forms the easternmost boundary of the Ogooue watershed (Séranne et al., 2008) (Figure 1a). On the shelf, recent fluviatile deposits consist of fine-grained sediments deposited at the mouth of the Ogooue River (Giresse and Odin, 1973). The wave regime along the Gabonese coast causes sediments to be transported northward. Sedimentary transport linked to longshore drift ranges between 300,000 m^3/yr. and 400,000 m^3/yr. (Bourgoin et al., 1963) and is responsible for the formation of the Mandji Island, a sandy spit of 50 km long located on the northern end of the Ogooue Delta (Figure 3). Except for the Cape Lopez Canyon, located just west of the Mandji Island with the canyon head in only 5 m water depth (Biscara et al., 2013), the Ogooue Fan is disconnected from the Ogooue Delta during the present-day high sea-level (Figure 3).

160
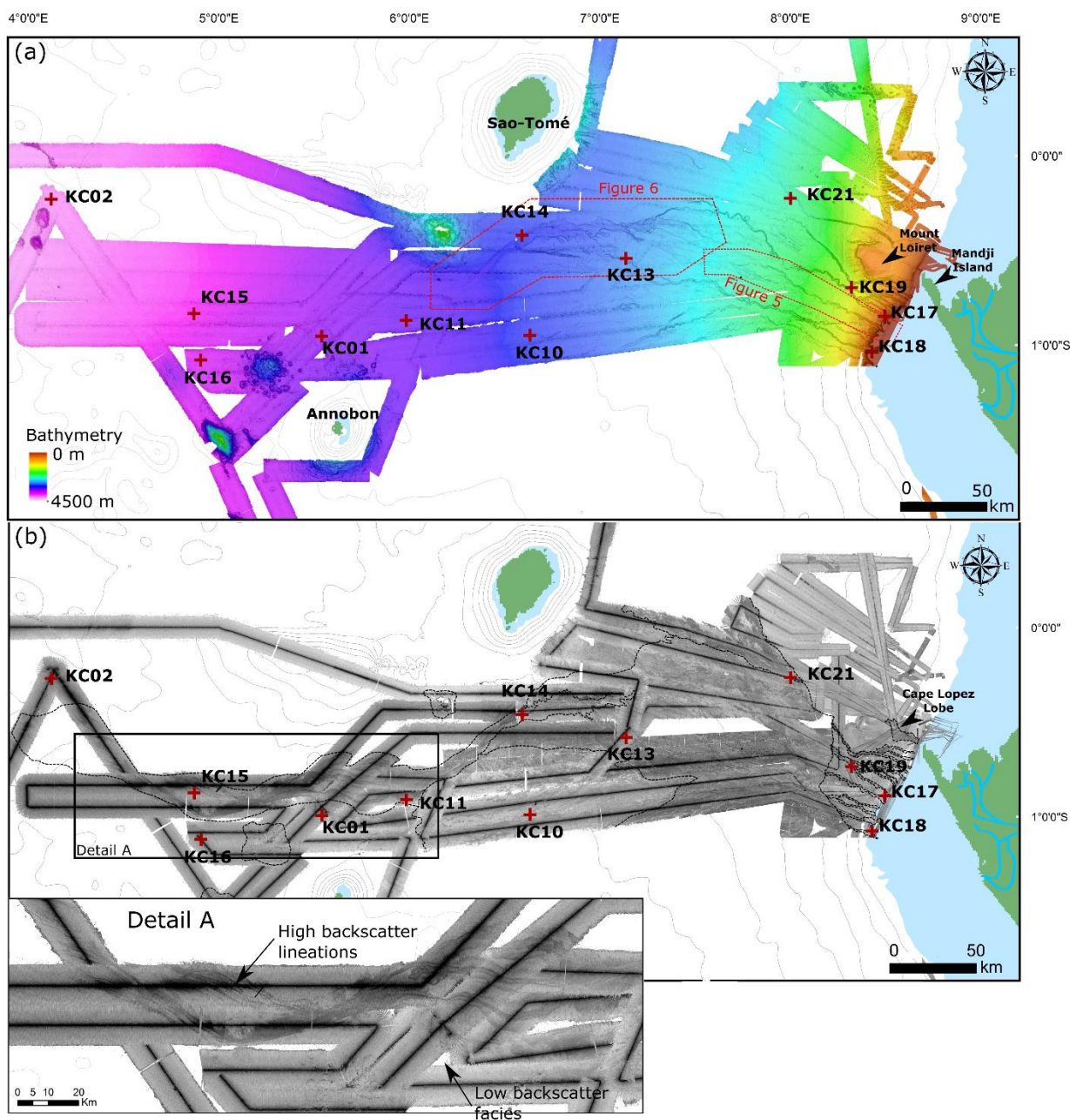
161 Figure 2: (a) Detailed bathymetric map of the Ogooue Fan, based on the multibeam echosounder data of the Optic
162 Congo2005 and MOCOSED2010 surveys. (b) Acoustic imagery of the Ogooue Fan (high backscatter: dark tones;
163 low backscatter: light tones). Detail A: close-up of the deepest part of the Ogooue Fan. Red crosses: location of the
164 studied cores.
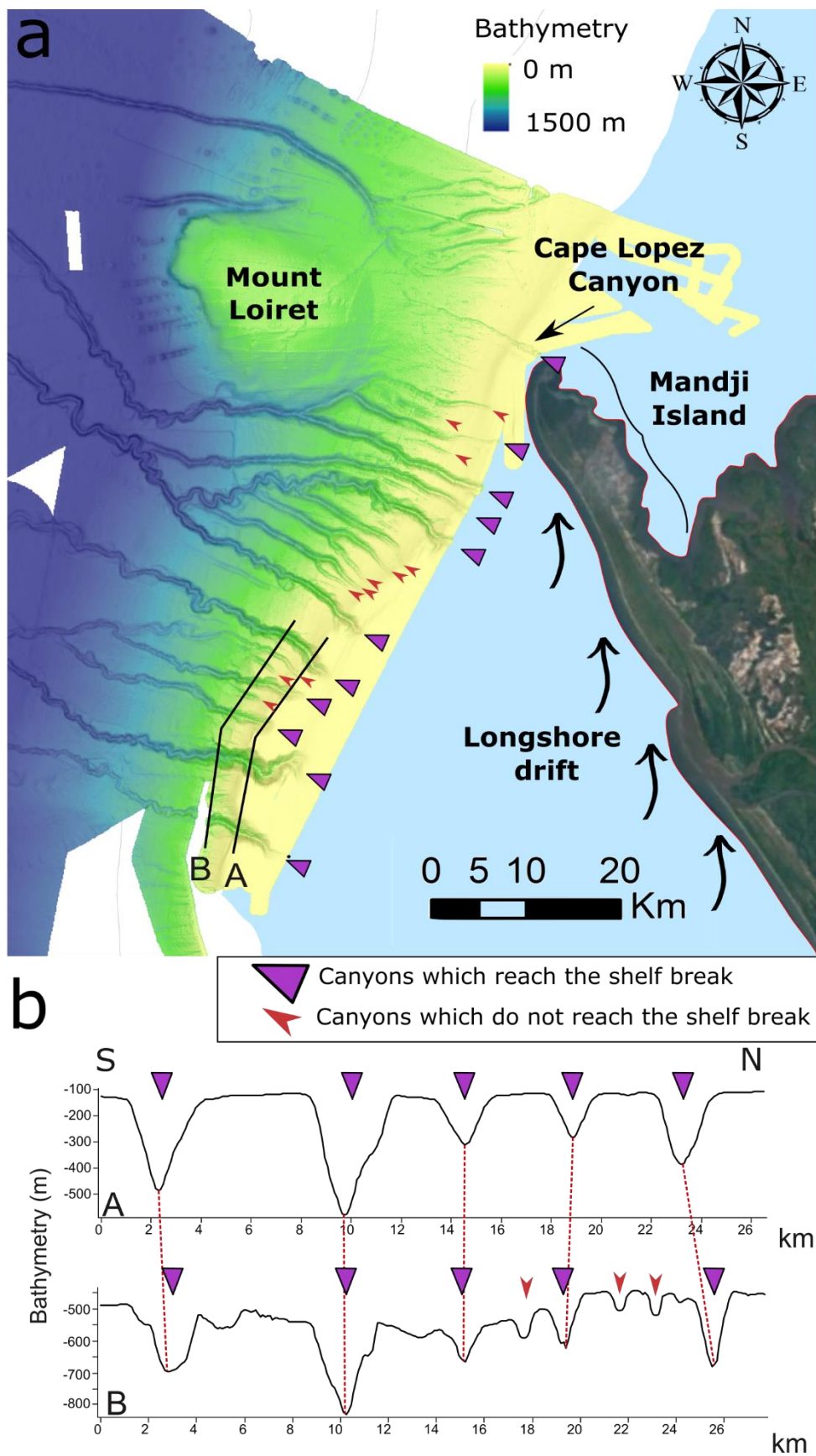
165
166 **Figure 3: a) Close-up view of the Gabon shelf and canyons ramp. Bathymetry is from the Optic Congo2005 and**
167 **MOCOSED2010 surveys, satellite view is from Google Earth. b) Two bathymetric profiles across the canyons**
168 **showing the two types of canyons which are present along the Gabonese slope.**

3 Material and method

The bathymetry and acoustic imagery of the studied area result from the multibeam echosounder (Seabat 7150) surveys conducted onboard the R/V "*Pourquoi Pas?*" and "*Beautemps-Beaupré*" during the MOCOSED 2010 and OpticCongo 2005 cruises (Mouscardes, 2005; Guillou, 2010) (Figure 2). The multibeam backscatter data (Figure 2b) have been used to characterize the distribution of sedimentary facies along the margin. Changes in the backscatter values correspond to variations in the nature, the texture and the state of sediments and/or the seafloor morphology (Unterseh, 1999; Hanquiez et al., 2007). On the multibeam echosounder images, lighter areas indicate low acoustic backscatter and darker areas indicate high backscatter. Five main backscatter types are identified on the basis of backscatter values and homogeneity (Figure 4). Facies A is a homogeneous low backscatter facies, Facies B is a low backscatter heterogeneous facies, and Facies C is a medium backscatter facies characterized by the presence of numerous higher backscatter patches. Facies D and E are high and very high backscatter facies, respectively. High backscatter lineations are present within Facies D.
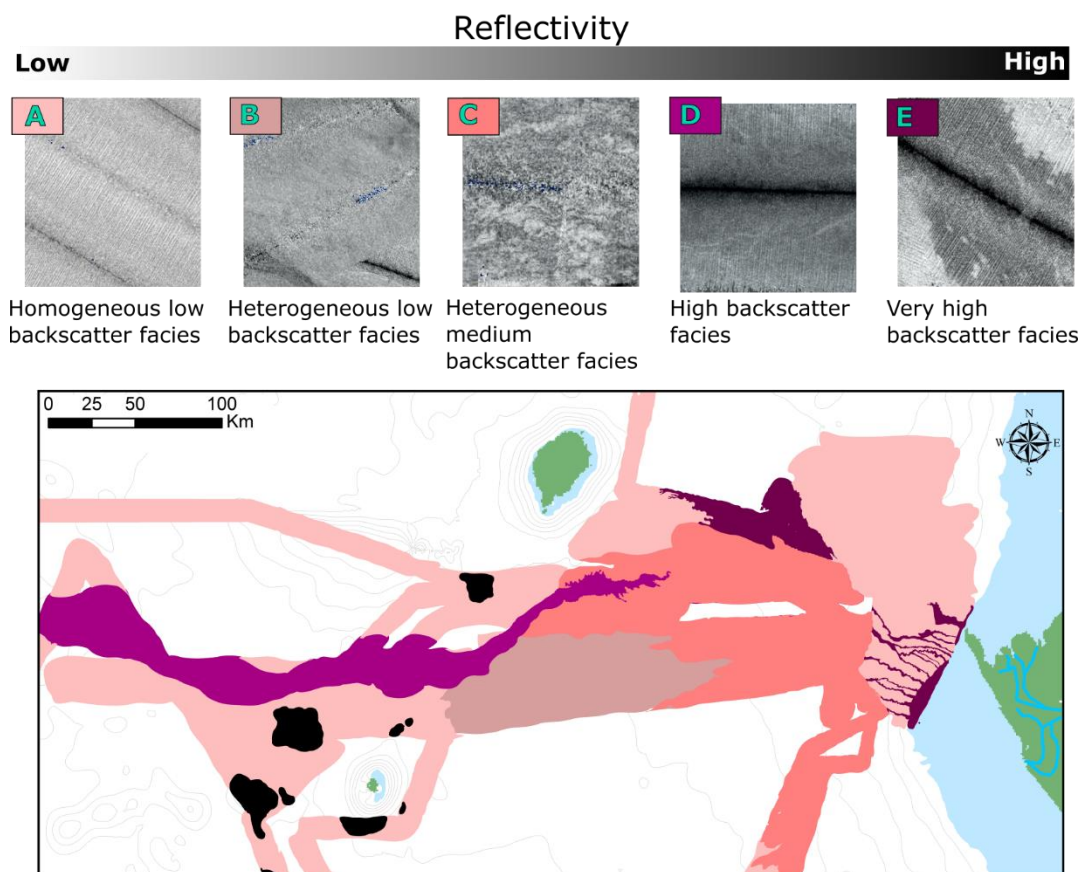
Figure 4 : Reflectivity facies map of the Ogooue Fan showing the five main backscatter facies.

A total of four thousand five hundred km of 3.5 kHz seismic lines were collected in the area of the Ogooue Fan during the MOCOSED 2010 cruise and 470 km during the Optic Congo 2005 cruise (iXblue ECHOES 3500 T7). These data were used to analyze the near-surface deposits. The dataset covers the shelf edge, the slope and the abyssal plain. In this study, the 3.5 kHz echofacies has been classified according to Damuth's methodology (Damuth, 1975, 1980a; Damuth and Hayes, 1977) based on acoustic penetration and continuity of bottom and sub-bottom reflection horizons, micro-topography of the seafloor and presence of internal structures.

The twelve Küllenberg cores presented here were collected during the cruise MOCOSED 2010. Five of these cores have already been presented in Mignard et al. (2017) (Table 1). Visual descriptions of the cores distinguished the dominant grain size (clay, silty clay, silt, and fine sand) and vertical successions of sedimentary facies. Thin slabs were collected for each split core section and X-ray radiographed using a SCOPIX

200 digital X-ray imaging system (Migeon et al., 1998). Subsamples were regularly taken
201 in order to measure carbonate content using a gasometric calcimeter and grain size using
202 a Malvern Mastersizer S. The stratigraphic framework is based on the previous work of
203 Mignard et al., (2017), new AMS ^{14}C dating (Table 1) done on core KC21 and KC18
204 and facies correlation to determine the boundary between Marine Isotopic Stage 1
205 (MIS1) and Marine Isotopic Stage 2 (MIS2). Indeed, the transition from MIS2 to MIS1
206 in the south-west Atlantic is marked by an abrupt increase in carbonate content (Volat
207 et al., 1980; Jansen et al., 1984; Olausson, 1984; Zachariasse et al., 1984). This feature
208 is recorded in all the cores of this study collected in the medium and distal part of the
209 system (Figure 5). The new AMS ^{14}C datings were realized on a mixture of different
210 planktonic foraminifer species living in the uppermost water column. Radiocarbon dates
211 have been calibrated using MARINE13 curve (Reimer, 2013) and using a standard
212 reservoir age of 400 years (Table 2; Mignard et al, 2017).

213

214 **Table 1: Characteristics of the twelve studied cores (MOCOSED 2010 cruise).**

Core	Depth (m)	Latitude	Longitude	Length (m)
KC01	3504	00°57,010' S	005°31,806' E	12,96
KC02	4109	00°13,525' S	004°07,620' E	12,76
KC10	3148	00°56,666' S	006°39,809' E	11,54
KC11	3372	00°52,008' S	006°00,008' E	9,92
KC13	2852	00°32,508' S	007°08,589' E	7,62
KC14	3140	00°25,010' S	006°36,006' E	11,34
KC15	3850	00°49,996' S	004°50,009' E	12,01
KC16	3738	01°05,003' S	004°52,010' E	11,48
KC17	565	00°51,188' S	008°29,377' E	8,20
KC18	366	01°01,940' S	008°25,409' E	7,99
KC19	1610	00°41,593' S	008°18,592' E	10,03
KC21	2347	00°13,004' S	008°00,011' E	11,81

215

216
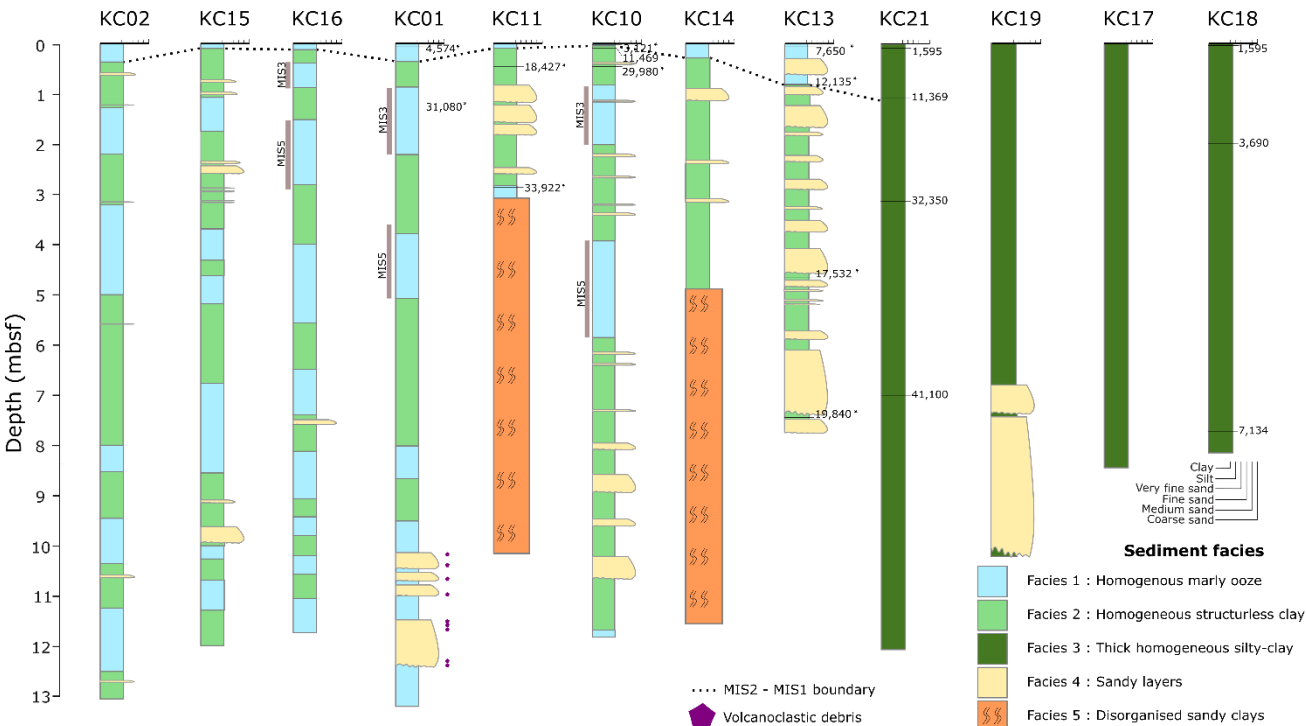
217

218 **Figure 5: Sedimentological core logs from the Ogooue Fan, showing grain-size variation, lithology and bed thickness**
219 **(locations of cores are presented in Figure 2). Ages are from ^{14}C dating (dates with a star are from Mignard et al.**
220 **(2017), grey bars show MIS3 and 5 sediments for KC16, KC01 and KC10 (Mignard et al., 2017).**

221

222 **Table 2: AMS ^{14}C ages with calendar age correspondences realized for this study (Reimer, 2013).**

Core number	Sample depth	Conventional age (reservoir correction) BP	Calendar age cal. BP
KC18	7	1,523 ±30	1,780
KC18	197	3,671±30	3,690
KC18	787	7056±40	7,134
KC21	12	1532±30	1,595
KC21	115	10,654±80	11,369
KC21	327	30,569±90	32,350
KC21	700	39,732±120	41,100

4   Results

4.1   Sedimentary facies

The classification in five sedimentary facies used here is based on photography and X-ray imagery, grain size analyses and $CaCO_3$ content (Figure 5). Interpretation of these facies is based on the comparison with previous sedimentary facies classifications such as Stow and Piper, (1984); Pickering et al., (1986) and Normark and Damuth, (1997).

Facies 1: Homogenous, structureless marly ooze. This facies is composed of structureless, light beige marly ooze with relatively high concentration of planktonic foraminifers. The mean grain size is around 15 µm and the $CaCO_3$ content ranges between 40 and 60%. This facies is interpreted as a pelagic drape deposit; it forms the modern seafloor of the deepest part of the Ogooue Fan and is observed in most of the core tops corresponding to the MIS 1 interval.

Facies 2: Homogenous, structureless clay: Facies 2 consists of dark brown clay. The mean grain size is less than 15 µm and the $CaCO_3$ content is less than 30%. This facies has been interpreted as hemipelagic drape deposits.

Facies 3: Thick, homogeneous silty-clay: Facies 3 consists of very thick homogeneous dark silt-clay layers containing less than 10% of $CaCO_3$. This facies contains numerous quartz and mica grains and plant debris indicating a continental origin of the sediments. It results from the deposition of the fine-grained suspended load coming from the Ogooue River and flowing down the slope or belonging to the flow tops of the turbidity currents.

Facies 4: Silty to sandy layers: Facies 4 consists of fine- to medium-grained sand beds with a thickness up to several meters. They are either normally-graded or massive and display a variety of bedding structures: ripple cross laminations, parallel laminations. The composition varies from terrigenous (quartz and mica) to biogenic (foraminifers), some sand beds are highly enriched in organic debris (Mignard et al., 2017). They are interpreted as being deposited by turbidity currents initiated on the Gabonese continental shelf. Four beds sampled at the base of core KC01 present a high

251 concentration of volcaniclastic debris, such particles are completely absent in all the
252 other sandy beds (Figure 5) sandy beds. This specific composition and the particular
253 location of the core both suggest that these sequences originate from the nearby
254 Annobon volcanic island.

255 *Facies 5: Disorganized sandy clays:* Facies 5 consists of thick intervals of deformed or
256 chaotic clay with deformed or folded silty to sandy layers containing mainly quartz
257 grains and rare plant debris. This facies is interpreted as a slump deposit or debrite.

4.2 Fan morphology

258
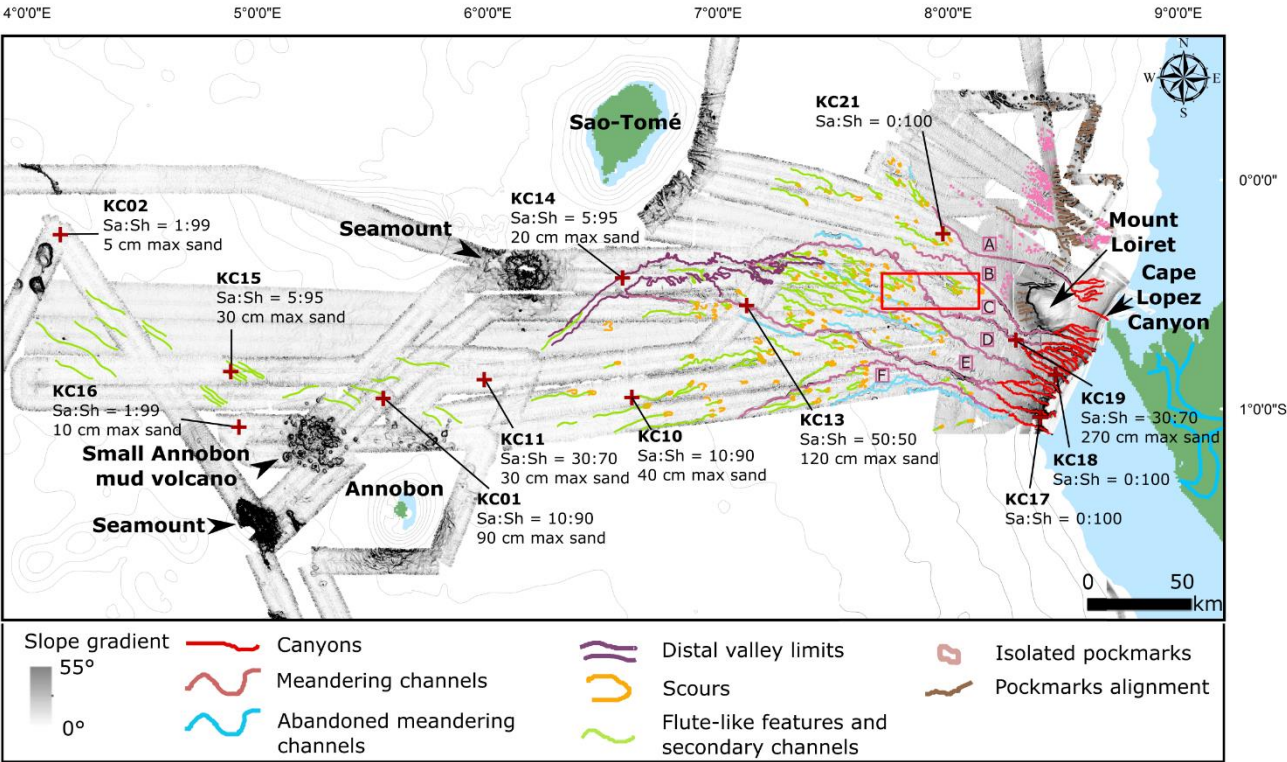
Figure 6: Interpreted gradient-shaded map of the Ogooue Fan showing the main features of the fan. A, B, C, D, E
and F are the six main channels discussed in the text. The sand/shale ratio of the cores are shown (Sa:Sh) as well as
the maximum sand-bed thickness in each core (max sand). A close-up view of the red rectangle is presented in
Figure 8.

264 Analysis of the seafloor data (bathymetry and acoustic imagery) reveals the different
265 domains of the Ogooue sedimentary system and the different architectural features of
266 the Ogooue Fan (Figure 6).

267 The Gabon continental shelf is relatively narrow, decreasing in width from 60 to 5 km
268 toward the Mandji Island (Figure 3). The slope is characterized by two main topographic
269 features: (1) the Mount Loiret, a guyot located just west of the Manji Island, which

forms a bathymetric obstacle on the upper slope and (2) a ramp of several tributary canyons located south of the Mount Loiret (Figure 3). This ramp is composed of several wide and deep canyons (several hundreds of meters deep and 2-3 km wide near the canyons head), with a "V-shape" morphology and which heads reach the shelf break. Several thinner and shallower incisions are located between these deep canyons. They are less than 100 m deep and 1 km wide and their heads are located between 200 and 400 m water depth (Figure 3). The continental shelf and the slope present low backscatter values except for the canyons, that correspond to very high backscatter value (Figure 4).

The transition between the continental slope and the continental rise, between 1,200 and 1,500 m water depth, is marked by a decrease in the slope gradient from a mean value of 2.3° to 0.9°. At this water depth, several canyons merge to form five sinuous channels (B to F in Figure 6). These channels appear with higher backscatter value than the surrounding seafloor (Figure 4). These sinuous subparallel channel-levees complexes extend down to 2,200 m water depth with a general course oriented toward the north-west (Figure 6 and 7). At 2,200 m water depth, the southernmost channel (channel F in Figure 6) deviates its path toward the south-west.

The sinuosity of these channels decreases Westward. Channel D sinuosity has been calculated over 2 km long segments (Figure 7C). It is less than 1.1 along the first 13 km corresponding to the canyon part. From 13 to 40 km d the mean sinuosity is 1.4 and then decreases to less than 1.2 between 40 to 90 km from the head. Finally, the most distal part of the channel, from 90 km from the head, is very straight with a sinuosity index lower than 1.1 (Figure 7C).
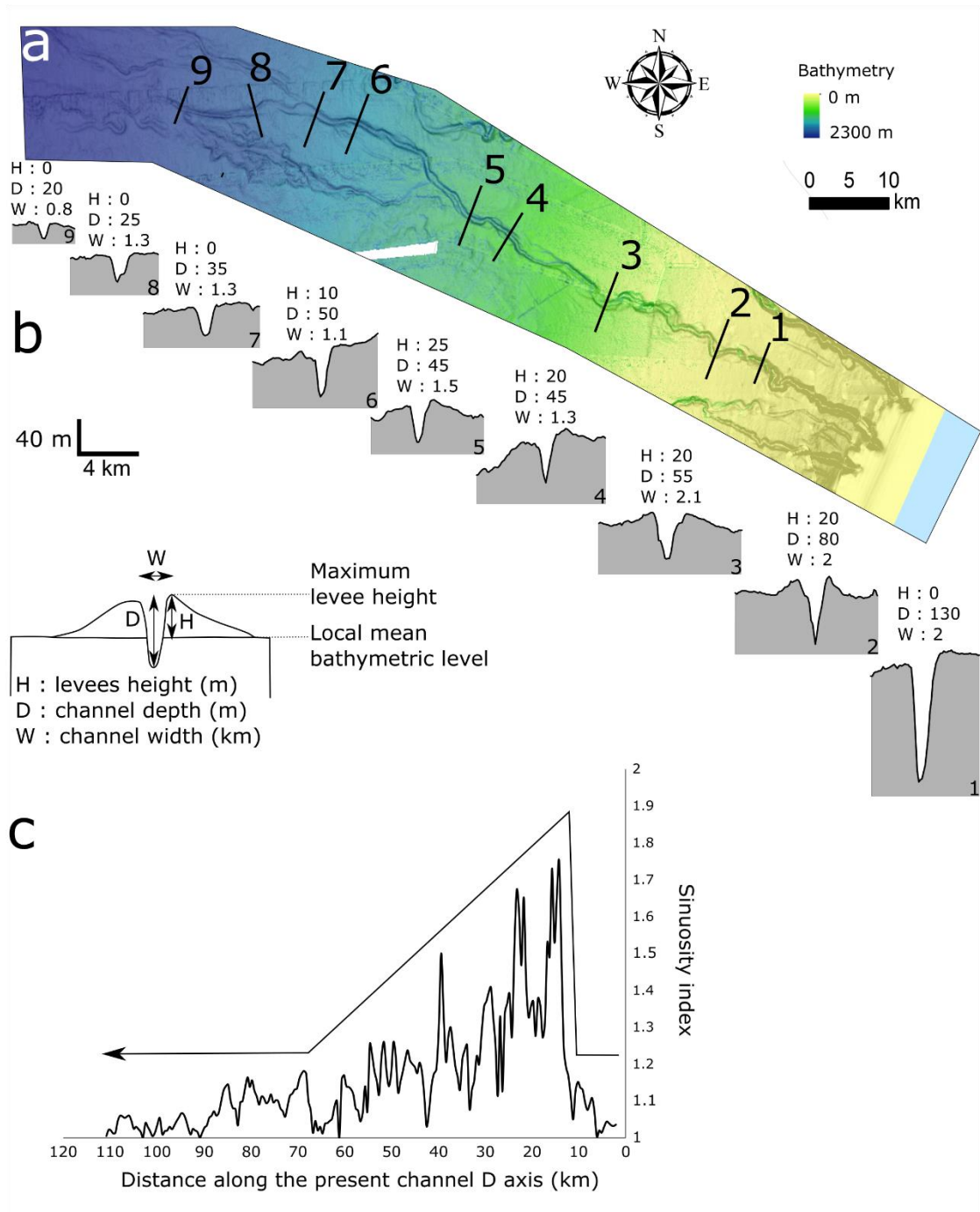
293
Figure 7: a) Detailed bathymetric map of channel D (location in Figure 2) b) serial bathymetric profiles showing the
294 **evolution of the channel-levees along the slope and c) sinuosity down the channel D measured along 2 km channel**
295 **segments.**
296
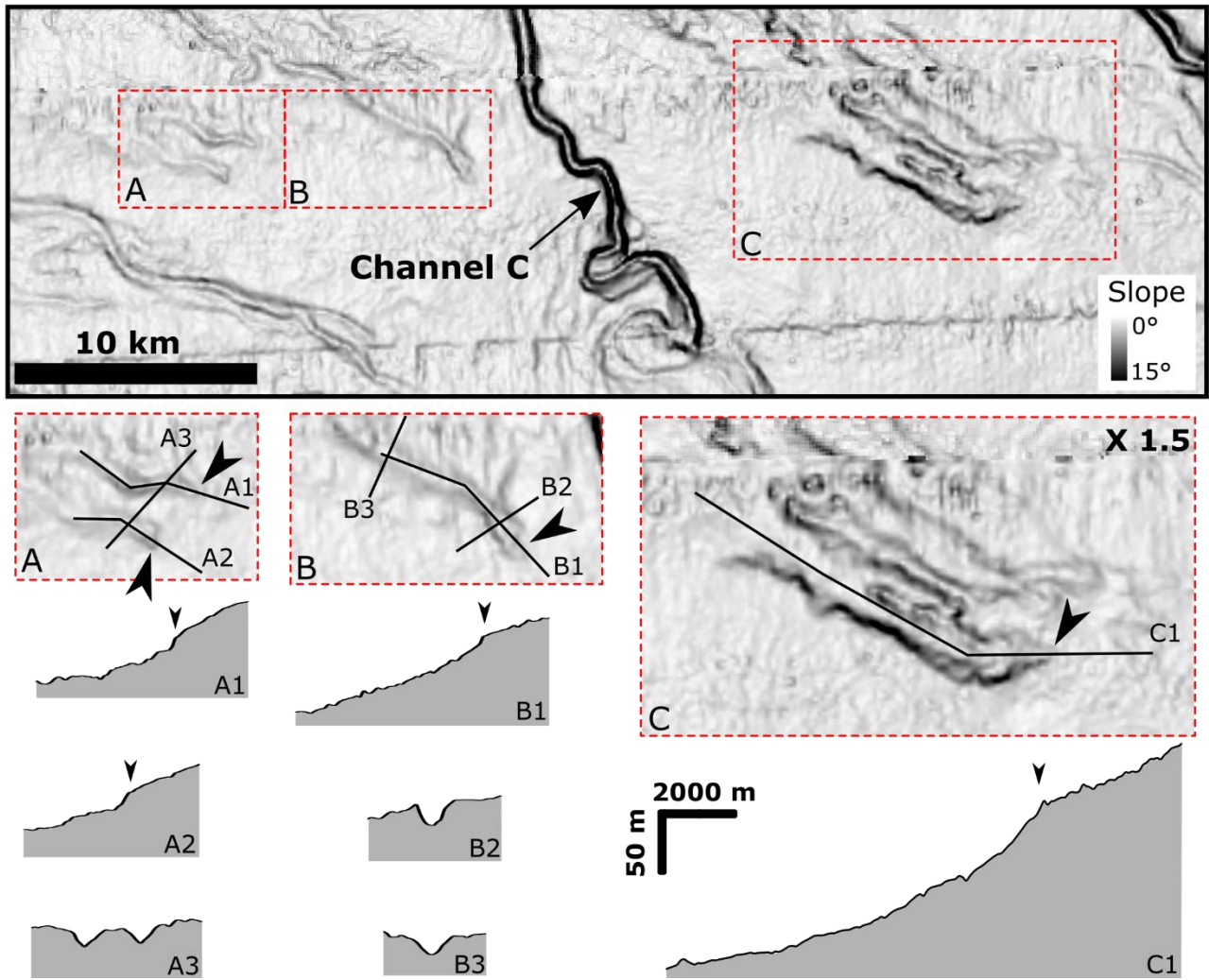
Figure 8: Close-up view of the gradient-shaded map showing erosional lineations (A and B) and amalgamated scours (C) in the central part of the system (location in Figure 6).

Downslope, in the central part of the system, the seafloor located between 2,200 m and 2,500 m water depth, presents numerous erosional features including scours, lineations and smaller, subsidiary channels, corresponding to channels with no headward connection with an obvious feeder system according to Masson et al. (1995) (Figure 8). These erosional features appear on a very gentle slope area (0.3°) characterized by a heterogeneous medium backscatter facies (Figure 4). At 2,500 m water depth, just south of the Sao-Tomé Island, the head of a large, 100 km long, mid-system valley appears (Figure 9). This valley can be subdivided in two parts of approximately equal length with two different orientations. The upper part of the valley is oriented E-W, whereas the lower part is oriented NE-SW. This direction change is due to the presence of a rocky seamount located north of the valley and which deflects its course. The upper part

311 of the valley is up to 15 km wide with numerous erosional scars and terraces on its

312 flanks. The valley bottom is characterized by very high backscatter value and small

313 internal erosion channels. Downstream, the valley becomes narrower with a "U" shape

314 (Figure 9, profile 5). Its flanks appear regular with no scar of down-flank mass deposits.

315 The depth of the valley decreases from 60 m in its central part to only 10 m near its

316 mouth. The area located south of the mid-system valley is characterized by a

317 heterogeneous low-backscatter facies. Some erosional features and subsidiary channels

318 are present but scarce.

319
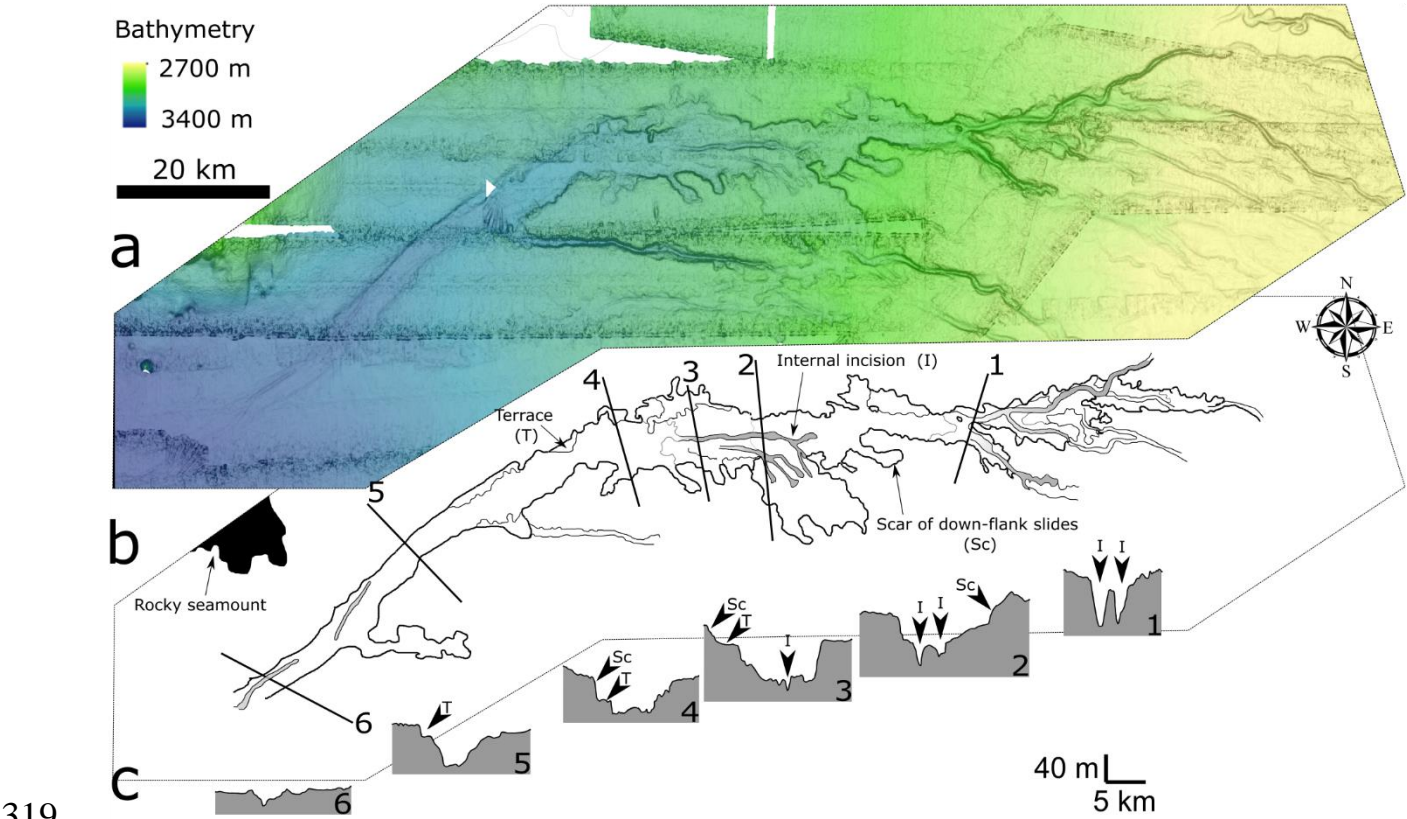
320 **Figure 9: (a) Detailed bathymetric map of the mid-system valley of the Ogooue Fan between 2,700 and 3,400 m**
321 **water depth; b) Interpretation of the main morphological features of the valley; c) Six transverse profiles of the**
322 **mid-system valley extracted from the bathymetry data (Sc: scar of down-flank slides, I: internal incision, T;**
323 **Terrace).**

324 West of the mid-system valley outlet, the seafloor is very flat and shows only subtle

325 morphological variations except for local seamounts. Few channel-like, narrow

326 elongated depressions (maximum 10 m deep) presenting high backscatter values can be

327 identified. These lineations are restricted to a long tongue of high backscatter at the

328 mouth of the valley (Figure 2b, Detail A). This tongue is globally oriented E-W at the

329   exit of the mid-system valley and then deflects toward the NW at 3,700 m water depth,

330   following the steepest slope.

331   North of Mount Loiret, the upper slope presents a lower slope gradient compared to the

332   south part and is characterized by the presence of numerous linear pockmark trains on

333   the upper part and pockmarks fields on the lower part. This whole area has a very low

334   and homogeneous reflectivity. Trace of active sedimentation on this part of the margin

335   is only visible in association with the Cape Lopez Canyon, which is the only canyon

336   located north of the Mount Loiret (Figure 3). This canyon is associated with a small

337   intraslope lobe located just north-east of the Mount Loiret and referred as the Cape

338   Lopez Lobe (Figure 10) (Biscara et al., 2011). This northern system continues

339   basinward with Channel A, the head of which is located in the vicinity of the Cape

340   Lopez Lobe. At 2,200 m water depth, Channel A ends and its mouth is associated on

341   the backscatter map with a fan-shaped area of very-high reflectivity, which is associated

342   with some subsidiary channels and erosional marks (Figure 4).

343
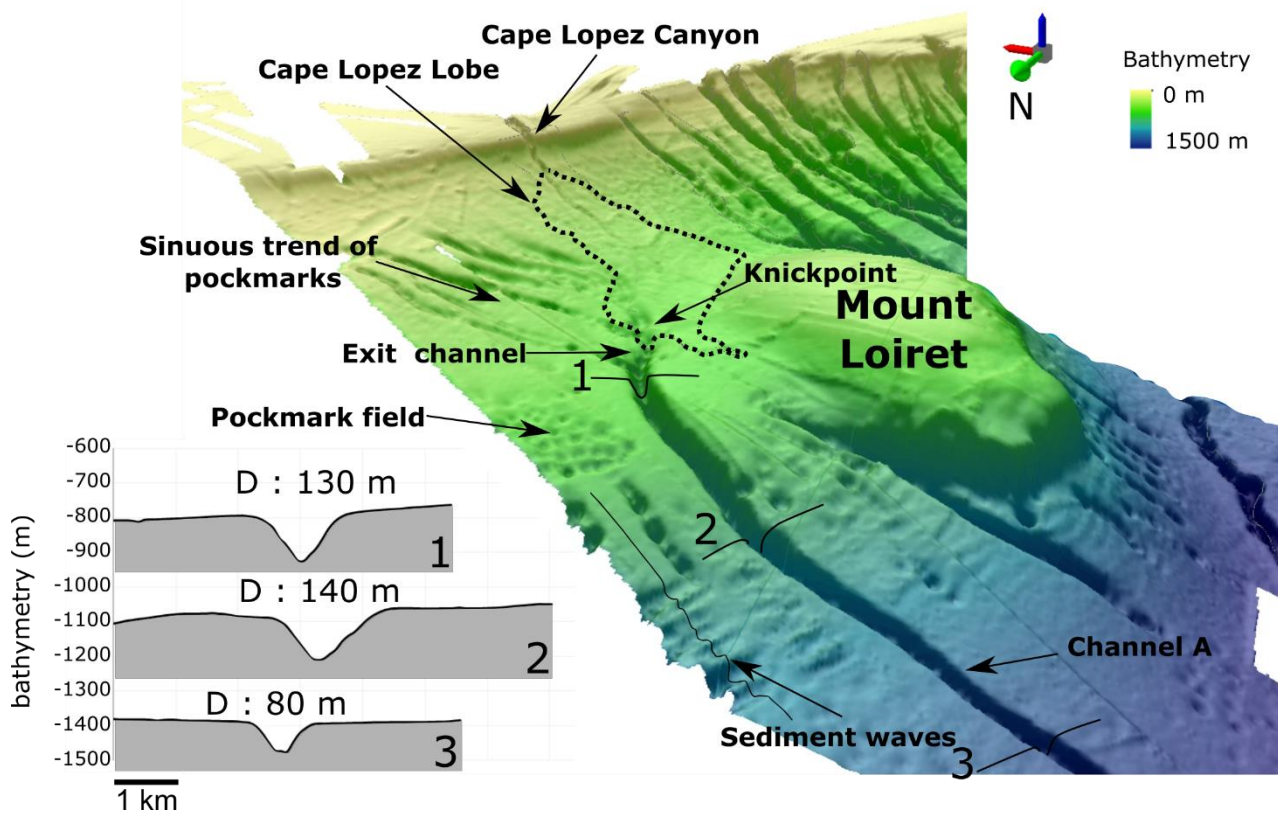
344 **Figure 10: a) Three-dimensional representation of the Cape Lopez, Canyon, Cape Lopez Lobe and Channel A, b)**
345 **three transverse profiles of Channel A.**

4.3 Echofacies analysis and distribution
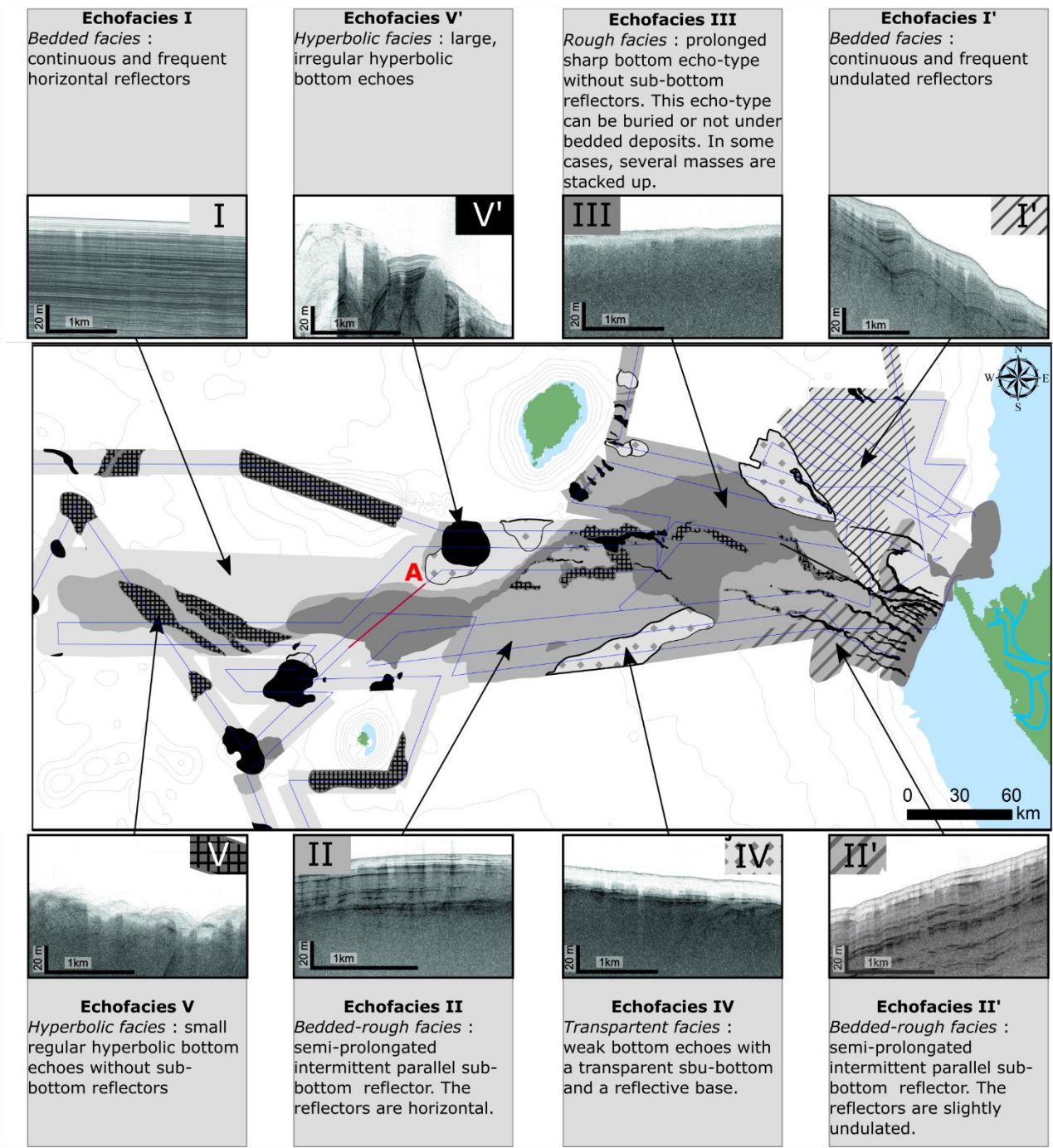
Figure 11: Echofacies map of the Ogooue Fan. Eight shades of grey represent the specific echofacies.

The main echofacies have been discriminated on the profiles based on amplitude, frequency and geometry of the reflections (Figure 11). They have been grouped into five main classes: (I) bedded, (II) bedded-rough, (III) rough, (IV) transparent and (V) hyperbolic. Most transitions between echofacies are gradual.

354 The echofacies of the edge of the Gabonese shelf consists of rough echofacies III (Figure
355 11). Core KC18 indicates that this area is dominated by fine-grained, structureless,
356 terrigenous sedimentation.

357 North of the Mount Loiret, the continental slope presents bedded echofacies I, which
358 evolves into echofacies I' down isobath 1,500 m which corresponds to an increase in
359 the slope gradient. Previous studies have shown that bedded echofacies are commonly
360 associated with alternating sandy and silty beds (Damuth, 1975, 1980a; Pratson and
361 Laine, 1989; Pratson and Coakley, 1996; Loncke et al., 2009) or with hemipelagic
362 sedimentation (Gaullier and Bellaiche, 1998). The very low reflectivity of the area and
363 the absence of any channel suggest that only hemipelagic sedimentation occurs in this
364 area. The wavy aspect of echofacies I' is certainly due to the post-deposition
365 deformation of the hemipelagic sediments (Bouma and Treadwell, 1975; Jacobi, 1976;
366 Damuth and Embley, 1979; Damuth, 1980b).

367 South of Mount Loiret, echofacies II and II' dominate on the continental slope. Despite
368 the lack of sampling, the presence of discontinuous seismic reflectors can indicate the
369 presence of coarse-grained sediment interpreted as turbidites (Damuth, 1975; Damuth
370 and Hayes, 1977). The echo-mapping of the continental rise reveals the presence of
371 different facies. The central part, just upstream of the mid-system valley, is
372 characterized by rough echofacies III that suggests the presence of a high proportion of
373 coarse-grained sediments. Some large channels are marked by hyperbolic facies
374 certainly due to the irregular and steep seafloor. South of the mid-system valley, facies
375 II dominates. Core KC10, collected in this area, indicates the alternation of clayey and
376 sandy layers but with a predominance of fine-grained sediments (Figure 5). Echofacies
377 IV is present in two main areas on the continental rise where they respectively form two
378 lobe-shaped zones: one on the northern part, following the limits of the high-reflectivity
379 area located at the mouth of channel A; the second in the southern part of the system in
380 association with channel F. This echo-facies commonly corresponds to structureless
381 deposits without internal organization due to mass-flow processes (Embley, 1976;
382 Jacobi, 1976; Damuth, 1980a, 1980b, 1994) but it can also characterize basinal fine-

383 grained turbidites (Cita et al., 1984; Tripsanas et al., 2002). Core KC21, collected in the

384 northern area indicates homogeneous silty-clay sediments with numerous detrital debris

385 similar to those collected near the continental shelf.

386
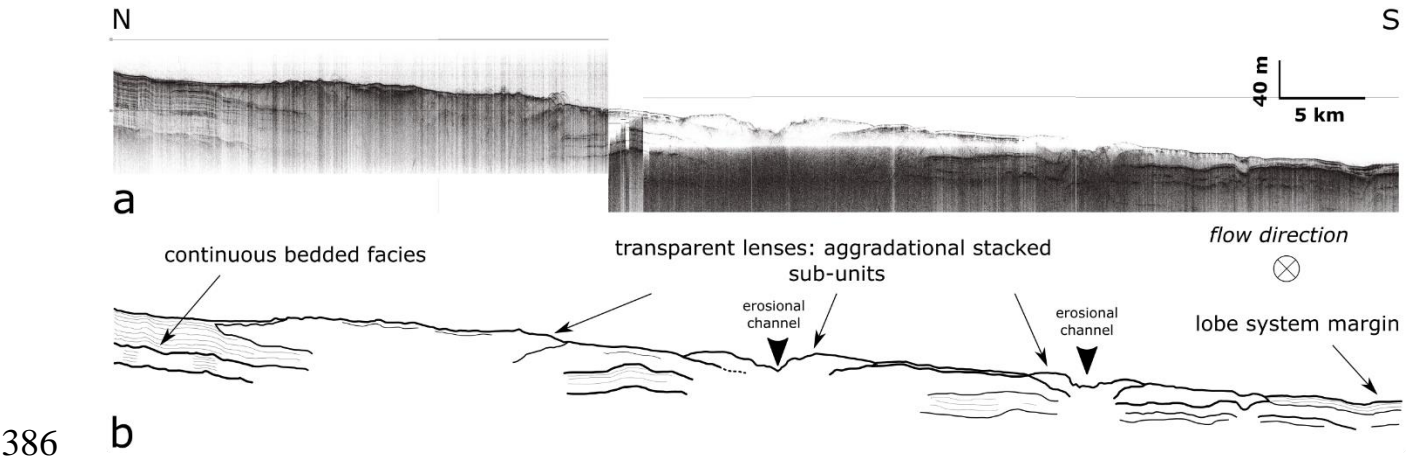
387

388 **Figure 12: a) Transverse 3.5 kHz very-high resolution seismic line and b) line drawing in the upper distal lobe area,**
389 **see Figure 11for location of the line.**

390 In the abyssal plain, the area of the elongated tongue noticeable on the backscatter data

391 presents different echofacies. Based on the 3.5 kHz profiles, it can be subdivided into

392 two main domains. The upstream part, at the outlet of the mid-system valley, is

393 characterized by rough echo character but with a specific organization: multiple

394 aggradational stacked transparent sub-units from 10 to 30 meters thick are visible on the

395 seismic lines (Figure 12). This organization is characteristic of sandy lobes deposits

396 (Kenyon et al., 1995; Piper and Normark, 2001). Core KC11, collected in this

397 environment, presents several decimeters-thick sandy layers and a several meter-thick

398 disorganized sandy-clay units interpreted as a slump. The downstream part presents

399 bedded-rough echofacies (II) associated with hyperbolic echofacies (V). Core KC15

400 intersected fine-grained sediments and several silty layers corresponding to the

401 distalmost turbidites.

402 On the edge of this tongue, high-penetration bedded facies (I) is dominant. The highly

403 continuous parallel bedding indicates hemipelagic sedimentation with no coarse-

404 grained fraction, which is confirmed by core KC16 and core KC02 both composed of

405 alternating carbonate-rich and carbonate-poor clay sediments. Facies V' forms some

406 patches on the seafloor and correspond to seafloor mounts. The hyperbolic facies is due

407 to the steep slopes and the irregular topography.

408 Facies V and IV are also present and form lenses around the island of Sao-Tomé and

409 Annobon. These features indicate some downslope sedimentary transfer from these

410 islands. The limited area covered by these facies suggests short transport by sliding.

411 **5   Interpretation and discussion**

412 **5.1   Sedimentary processes along the fan**

413 The Ogooue Fan is a delta-fed passive margin deep-sea mud/sand-rich submarine fan

414 according to the classification of Reading and Richards (1994). However, analysis of

415 sub-surface data (bathymetry, acoustic imagery and 3.5 kHz echo-characters) reveals a

416 great variability of sediment processes in the different domains of the margin, controlled

417 by variations in slope gradient and the presence of seamounts (Figure 13a).

418
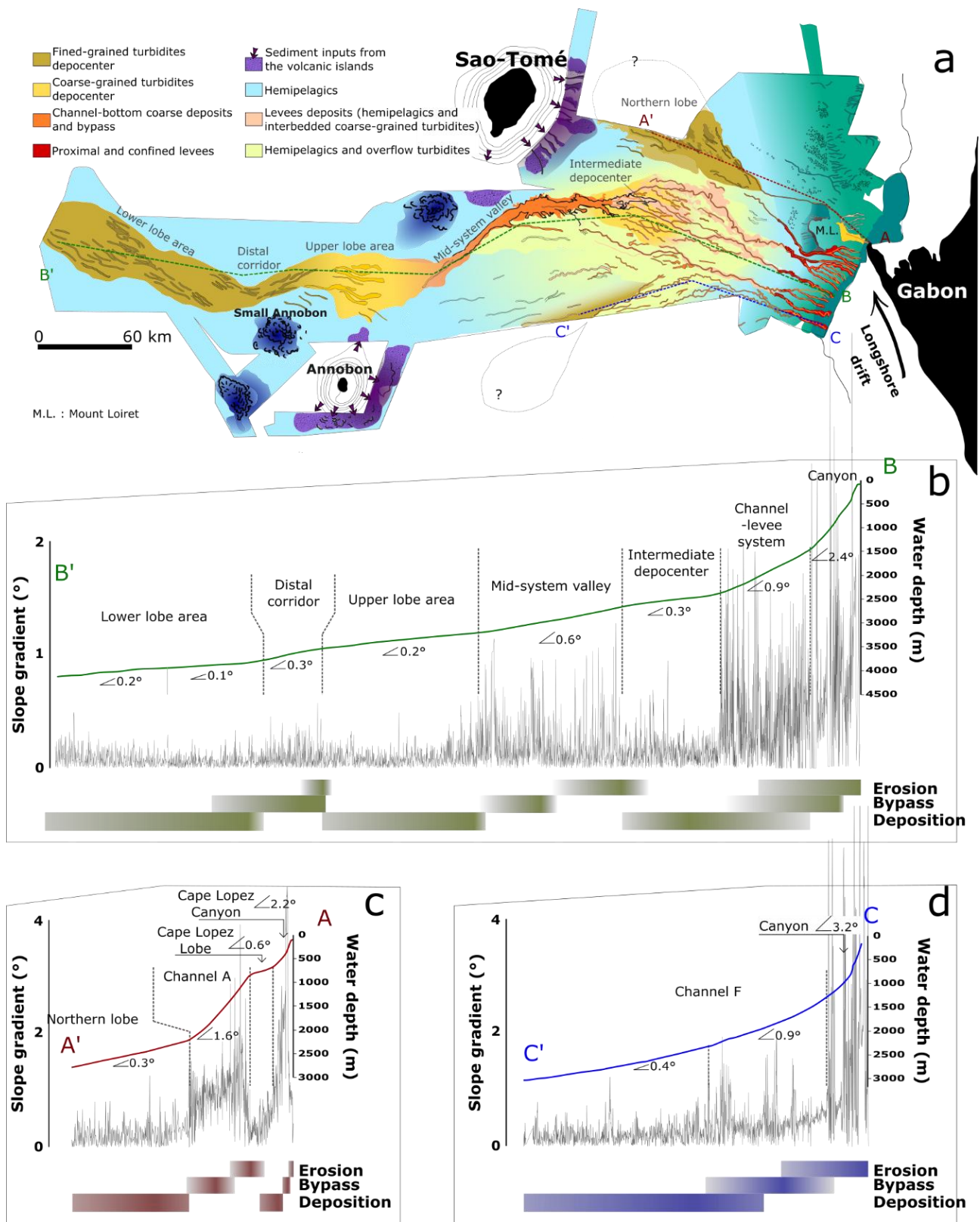
Figure 13: a) Synthetic map showing the architecture and the recent sedimentary processes of the Ogooue Fan
determined by imagery and echofacies mapping; b) c) and d) Longitudinal profiles from the bathymetric data along
the central, northern and southern part of the Ogooue Fan and slope gradient (in degree, measured every 100m).
The differences in slope gradient along the transects are associated with the main sedimentary processes
encountered along the slope.

5.1.1 Canyons system

Erosional processes predominate on the upper part of the slope as indicated by the presence of numerous tributary canyons (Figure 3). Based on the comparison of the canyon depths, widths and head positions, we observe the existence of two types of canyons as described in Jobe et al. (2011) along the Equatorial Guinea margin. The canyons presenting a deep (> hundreds of meters deep) "V" shape and which indent the shelf edge are type I canyons (*sensu* Jobe et al., 2011), whereas the shallower canyons (<100 m deep) with a "U" shape and which do not indent the shelf are type II canyons (*sensu* Jobe et al., 2011). The difference between these two types of canyons indicates different initiation and depositional processes. Type I are commonly associated with high sediment supply and the canyons initiation and morphology are controlled by sand-rich erosive turbidity currents and mass-wasting processes (Field and Gardner, 1990; Pratson et al., 1994; Pratson and Coakley, 1996; Weaver et al., 2000; Bertoni and Cartwright, 2005; Jobe et al., 2011). In contrast, Type II canyons are found in areas of low sediment supply. Their initiation is attributed to retrogressive sediment failures and subsequent headward erosion (Shepard, 1981; Twichell and Roberts, 1982; Stanley and Moore, 1983). Their evolution is controlled by depositional processes involving fine-grained sediments - hemipelagic deposition and dilute turbidity currents - that can be carried over the shelf and upper slope into the canyon heads but without significant erosion (Thornton, 1984). North of the Mount Loiret, the fine-grained sedimentation has completely infilled several type II canyons creating sinuous trains of pockmarks. These pockmarks have been previously described in Pilcher and Argent (2007). Variations in the localisation of coarse-grained sediment supplies play a key role on the development of the two types of canyons. Along the central Gabonese shelf, the very recent development of the Mandji Island 3,000 years BP (Giresse and Odin, 1973; Lebigre, 1983) favoured the construction of the Cape Lopez Type I canyon, which is presently active (Biscara et al., 2013).

5.1.2 Channels system

The transition from canyons to sinuous channels with external levees (*sensu* Kane and Hodgson, 2011) is related to a decrease in slope gradient from the continental slope (> 2°) to the continental rise (< 1°). The sinuous channel-levees systems develop on a relatively gentle slope (0.9°) from 1,500 to 2,200 m water depth. These channels are mainly erosive in their axial part (Normark et al., 1993) while deposition occurs on low-developed external levees (25 m maximum levees height for channel D; Figure 7). The external levees of the four central channels (B, C, D and E in Figure 2) show high reflectivity that suggests frequent turbidity currents overspill. These channels are deeply incised in the seafloor (average 70 m deep for channel D and 90 m deep for channel A; (Figure 7 and Figure 10) below the associated levees, when present. This feature is similar to the modern Congo Channel (Babonneau et al., 2002) and is opposed to the morphology of aggrading channels (such as the Amazon Channel) where the thalweg is perched above the base of the levees system (Damuth, 1995). This entrenched morphology prevents extensive overflow of turbidity currents and is the probable cause of low development of external levees and inhibits channel bifurcation by avulsion. It has been proposed for the Congo Channel that the entrenched morphology of the channel confines the flow and keeps the energy high enough to allow a transport of sediment to very distant areas (Babonneau et al., 2002).

Several studies have documented that sinuosity of submarine channels increases with time (Peakall et al., 2000; Babonneau et al., 2002; Deptuck et al., 2003, 2007; Kolla, 2007). The sinuous upper parts of the channels (1.3 < sinuosity < 1.75 for channel D; Figure 7C) have consequently undergone a long history whereas the distal straighter parts of the channels are in a more immature stage. Moreover, the height of the external levees and the depth of the channels both decrease in the lower parts of the channels system (Figure 7). These morphological changes are due to a slope gradient decrease (< 0.5° from transect 6 along channel D; Figure 7) that progressively slows down the flow velocity and reduces its erosional power. Simultaneously, deposition of fine particles by spilling of the upper part of the flow on the external levees leads to a

480 progressive decrease of the fine-grained fraction transported by the channelized flows

481 (Normark et al., 1993; Peakall et al., 2000).

482 At 2,200 m water depth, the appearance of numerous erosional features such as isolated

483 and amalgamated spoon–shaped scours (Figure 8 C1), erosional lineations and

484 subsidiary channels with limited surface expression (10-20 m deep, Figure 8 B2, B3)

485 are characteristic of the channel lobe transition zone (Figure 8) (Kenyon et al., 1995;

486 Wynn et al., 2007; Jegou et al., 2008; Mulder and Etienne, 2010). The appearance of

487 these features correlates with a second abrupt decrease in slope gradient (from 0.9° to

488 0.3°) and with the transition from bedded-rough to rough echo-facies indicating a

489 change in the sedimentary process. This area corresponds to deposition by spreading

490 flows in an unchanneled area referred as the intermediate depocenter in Figure 13 and

491 covering area surface of ca. 4,250 km². However, the low penetration of the 3.5 kHz

492 echosounder and the limited number of seismic lines in this area did not allow a more

493 detailed interpretation of the sedimentary processes in this part of the system.

494 5.1.3 Mid-system valley and distal lobe complexes

495 The presence of a steeper slope downslope of the intermediate depocenter (0.6°) led to

496 the incision of the mid-system valley, which acts as an outlet channel for turbidity

497 currents that are energetic enough to travel through the flatter depositional area (Figure

498 13b). The upstream part of the valley is multi-sourced and has migrated upstream by

499 retrogressive erosion, whereas the downstream part appears more stable with a straighter

500 pathway and steeper flanks, these features being similar to the Tanzania Channel

501 described by Bourget et al. (2008). The pathway of the valley seems to be controlled by

502 the seafloor topography as the valley deviates near the rocky seamount located west of

503 Sao-Tomé. This large mid-system valley corresponds to a single feeding "source" for

504 the lower fan and, consequently, the final depositional area is located downstream of

505 the valley.

506 At the outlet of the mid-system valley, the echofacies shows an area mainly

507 characterized by rough echofacies (III) forming stacked lenses. This area, referred as

508 the upper lobe area in Figure 13, constitutes the main lobe complex (*sensu* Prélat and

509 Hodgson, 2013) of the Ogooue Fan. According to the seismic data, the depositional area

510 of the lobe complex is ~ 100 km long, reaches ~ 40 km in width, spreads over 2,860 km²

511 and reaches up to 40 m in thickness. The transparent lenses are interpreted as lobe

512 elements and seem to be bounded by erosive bases (Mulder and Etienne, 2010). Some

513 incisions (< 15 m deep) are imaged on the top surface of the lobes; two of them are

514 visible in Figure 12. The area where incisions are present is interpreted as the

515 channelized part of the lobe. This lobe area presents a gentle slope (0.3°) oriented north-

516 south, suggesting that topographic compensation would shift future lobe element

517 deposition southward. However, the few numbers of seismic lines do not allow the

518 precise internal geometry and the timing of the construction of the different lobe units.

519 This depositional area is not the distalmost part of the Ogooue Fan. West of this lobe,

520 evidences of active sedimentation are visible on the reflectivity map (Figure 2, Figure

521 4). The reflectivity map shows high-backscatter finger-shape structures suggesting

522 pathways of gravity flows (Figure 2b, detail A). These lineations (< 10 m deep) are

523 concentrated in a 20 km wide corridor just west of the lobe area and then form a wider

524 area extending up to 550 km offshore the Ogooue Delta. This part of the system follows

525 the same scheme as the one previously described between the intermediate depocenter

526 and the upper lobe area (Figure 13b). The corridor appears on a segment of steeper slope

527 (0.3°) just at the downslope end of the upper lobe area (0.2°). This corridor, which

528 disappears when the slope becomes gentler (0.1°), was certainly formed by the repeated

529 spill-over of the fine-grained top of turbidity currents over the upper lobe area. This

530 architecture suggests that this corridor is dominated by sediment bypass (*sensu*

531 Stevenson et al., 2015). On the most distal segment with a very low slope gradient (0.1-

532 0.2°) sediment deposition dominates.

533 **5.1.4 Isolated systems**

534 On the northern part of the slope, the isolated system composed of the Cape Lopez

535 Canyon, Cape Lopez intraslope lobe, channel A and northern lobe follows the same

scheme (Figure 13c). Cape Lopez Canyon terminates at 650 m water depth at an abrupt decrease in slope gradient (from more than 1.7° to 0.6°) caused by the present of the Mount Loiret (Figure 10). The Cape Lopez intraslope lobe occupies a small confined basin, 6 km wide and 16 km long and covers an area of 106 km². This lobe appears very similar with the "X fan" described in Jobe et al. (2017) on the Niger Delta slope (8 km x 8 km, 76 km²) and is in the same size range as the intraslope complexes studied in the Karoo Basin by Spychala et al. (2015) (6-10 km wide and 15-25 km). The two successive depositional areas, composed by the Cape Lopez lobe and the northern lobe, are located on areas with a low slope gradient (0.6-0.3°) whereas erosion and sediment bypass dominate on segments of steeper slope gradient (1.6°). The high slope gradient between the two depositional areas favored the construction of a straight deeply entrenched channel (>100 m deep near the knickpoints) without levee (Figure 7b) instead of a large valley similar to the central mid-system valley.

In the southern part of the fan, channel F transports sediments southward (Figure 13d). At 2,200 m water depth, a transparent echofacies appears associated with the pathway of this channel. This echofacies suggests that sediment transported by this channel might be partly deposited in this area by turbidity current overflow. This channel might also be associated with a depositional lobe; however, the area covered by the MOCOSED survey does not allow us to image it.

5.2   The Ogooue Fan among other complex slope fans

The Ogooue Fan develops on a stepped-slope (Prather, 2003) which creates a succession of depositional areas on segments with gentle slope (referred as 'steps' in Smith, (2004)) and segments of steeper slope ("ramps" in Smith, 2004) associated with erosion or sediment bypass (Figure 13) (Demyttenaere et al., 2000; O'Byrne et al., 2004; Smith, 2004). The depositional behavior in these systems is guided by an equilibrium profile of the system that forms preferential areas of sedimentation or erosion (Komar, 1971; Ferry et al., 2005). As described in the conceptual model of O'Byrne et al. (2004), erosion is favored where local gradient increases, the eroded sediments being delivered

downstream resulting in a local increase in sediment load (O'Byrne et al., 2004; Gee and Gawthorpe, 2006; Deptuck et al, 2012). This kind of fan geometry is common along the West African margin where abrupt changes in slope gradient and complex seafloor morphology are inherited from salt tectonic movement (Pirmez et al., 2000; Ferry et al., 2005; Gee and Gawthorpe, 2006; Gee et al., 2007). Deptuck (2012) has described the influence of stepped-slope on sedimentary processes along the western Niger Delta. He showed that differences of slope gradient between ramps (0.8° to 2.1°) and steps (0.3° to 1.1°) induce the transition from vertical incision and sediments removal to preferential sediments accumulation (Deptuck et al., 2007; Deptuck, 2012). Gradient changes along the Gabonese margin are however lower than the ones reported in Deptuck, (2012) and variation in slope gradient of 0.2° appears to be enough to modify sedimentary processes. The impact of subtle changes of slope gradients has already been highlighted by studies of the Karoo basin (Van der Merwe et al., 2014; Spychala et al., 2015; Brooks et al., 2018) and Moroccan margin where sedimentary processes are controlled by very subtle gradient changes (<0.1°) (Wynn et al., 2012

Moreover, in the case of the modern Ogooue Fan, and conversely to what is observed in the Congo and Niger systems, the presence of several bathymetric highs including the volcanic islands of the CVL and the Mount Loiret constitutes additional stresses for the flows and creates a more complex slope profile. These bathymetric highs induce a lateral shift of the pathways of different channels as well as the pathway of the mid-system valley and form several downslope depositional lobes such as the Cape Lopez lobe that is constrained by the presence of the Mount Loiret. Several complex-slope systems have already been described in the literature with slope complexity due to salt-related deformations (e.g. Gulf of Mexico (Prather et al., 1998; Beaubouef and Friedmann, 2000), offshore Angola (Hay, 2012) or basin thrusting (offshore Brunei; McGilvery and Cook, 2003, Markan margin; Bourget et al., 2010). For these systems, the slope evolves rapidly, and sedimentation and erosion are unlikely to establish an equilibrium profile. In contrast, the Gabonese margin reached a mature evolutionary stage with only weak and slow salt tectonic activity (Chen et al., 2007), and

sedimentation and erosion certainly dominate the short-term evolution of the slope. The Ogooue Fan appears to be much more similar to the morphology of the Northwest African margin where the Madeira, the Canary and the Cape Verde islands create a complex slope morphology along the Moroccan and Mauritanian margin (Masson, 1994; Wynn et al., 2000, 2002, 2012).

5.3 Sedimentary facies distribution

The main processes involved in the deposition of the Upper Quaternary sediments of the Ogooue Fan are pelagic and hemipelagic suspension fall-out together with turbidity currents. Fine-grained pelagic/hemipelagic 'background' sedimentation is dominant across a large area of the margin, particularly on the lower rise and the adjacent basin plains. These sediments are then overprinted by downslope gravity flows such as turbidity currents. However, the previously described fan organization implies a specific distribution of the sedimentary facies and grain-size distribution within the system (Figure 6).

Cores collected in the upslope area (KC18 and KC17) show mostly hemipelagic sediments with a very low carbonate content. This reflects significant detrital flux associated with proximity to the Ogooue platform and the influence of the Ogooue river plume. Core KC19 collected down the slope just at the transition from canyon to channel-levee complexes show two several meters-thick sandy successions corresponding to top-cut-out Bouma sequences (Ta) interbedded with the upper slope hemipelagites. These sandy turbidites, which are the thickest sand beds recorded in all the cores (Figure 6), indicate the occurrence of high-density turbidity currents flowing down the canyons. The lack of the upper parts of the turbidite is consistent with deposition in the canyons of coarse-grains located at the base of the turbidity currents, whilst the finer upper part of the current is transported downstream and/or spills over the external levees. External levee deposits have been sampled by core KC13, which shows numerous turbidites made up of centimeter-thick, fining upward, parallel or ripple cross-laminated of silt and fine sands (Figure 5). Unfortunately, no core has been

621 collected directly in the intermediate depocenter. However, the rough echofacies III
622 found in this area associated with various erosional features both suggest a high
623 sand/mud ratio.

624 The mid-system valley acts as a conduit for the sediments coming from the upper part
625 of the system, transporting them further downstream. However, the sediments resulting
626 from the erosion of this valley constitute certainly a part of the sediments deposited in
627 the lobe complex area. According to the available bathymetric data, the volume of
628 sediment removed from the mid-system valley is between 8 and 10 km^3. We assume
629 that these sediments are mainly fine-grained due to the deep location of the valley. Core
630 KC14, collected on an internal terrace of the valley, shows that this valley is also an
631 area of active sedimentation notably due to down-flank sliding. The bottom of the valley
632 comprises slump deposits and coarse-grained sediments deposited by gravity flows
633 coming from the upper part of the system.

634 Downstream of the mid-system valley, core KC11 show that coarse-grained turbidity
635 currents are deposited in the proximal part of the lobe complex. The abrupt transitions
636 between erosional/bypass and depositional behavior observed notably at the mouth of
637 the mid-system valley is the result of hydraulic jumps affecting flows when they become
638 unconfined between channel sides and spread laterally (Komar, 1971; Garcia and
639 Parker, 1989). Core KC15, located in the lower lobe area, is composed of very thin silty
640 turbidites corresponding to the upper parts of the Bouma sequence interbedded with
641 hemipelagic deposits. The upper lobe acts as a trap for the basal sand-rich parts of
642 gravity flows. Consequently, only the upper part of the flows, which is composed of
643 fine-grained sediments, travels beyond this area. The spatial distribution of facies
644 suggests a filling of successive depocenters with a downslope decrease of the coarse-
645 grained sediment proportion (Figure 6). The same facies distribution can be observed in
646 the northern system. No sandy turbidites are recorded in KC21 located in the Northern
647 lobe, only fine-grained sedimentation, whereas the study of cores taken in the Cape
648 Lopez lobe shows the presence of numerous sandy turbidites (Biscara et al., 2011). The
649 Northern lobe is thus fed by the downslope flow stripped suspended fines transported at

the top of turbidity currents flowing through the Cape Lopez Canyon, similarly to intraslope lobes observed in other locations (e.g. Spychala et al., 2015; Jobe et al., 2017). Whatever the current pathways are, the deposited material has a continental origin as suggested by the abundance of quartz, micas and plant debris in the coarse-grained fraction. The important proportion of planktic foraminifers in the coarse-grained fraction of turbidites located in the distal part of the system (core KC10- KC11- KC15) suggests that turbidity currents previously entrained pelagic and hemipelagic deposited upslope where such deposits cover large areas (Viana and Faugères, 1998). The presence of volcanoclastic debris in a sandy layer found at the base of core KC01 suggests that sedimentary input may also come from the volcanic islands of Sao Tomé or Annobon. However, acoustic data indicate that these inputs are limited to the close vicinity of the Sao-Tomé and Annobon islands. In contrast to the model proposed by Wynn et al., (2000) for the Northwest African slope, the volcanic islands and other seamounts present on the Ogooue Fan act mainly as obstacles for the flow pathway but are not important sediment sources for the fan.

5.4 Palaeoceanographic control on the fan activity

The results of Mignard et al. (2017) concerning the study of five cores located along the central part of the Ogooue Fan showed that the fluvial system fed the fan with sediments almost only during times of relative low sea-level. This relative sea-level control on turbidite activity (switch on/off behavior) is classical for mid and low latitude passive margin fans where canyon heads are detached from terrestrial sediment sources (e.g. Mississippi Fan (Bouma et al., 1989), Amazon Fan (Flood and Piper, 1997), Rhone Fan (Lombo Tombo et al., 2015), Indus Fan (Kolla and Coumes, 1987). Conversely, sedimentation during periods of relative high sea-level such as the Holocene, is dominated by hemipelagic to pelagic fall-out with a low part of fine terrigenous particles. Therefore, all cores collected in the central part of the system are capped by 8 to 20 cm of light-brown nannofossil ooze corresponding to Holocene hemipelagites (Figure 5).

678   However, the northern part of the system appears to have a different behavior. Biscara
679   et al., (2011) showed that the Cape Lopez lobe is currently recording both hemipelagic
680   and turbidity current sedimentation despite the present-day high sea-level. This lobe is
681   fed with sediment from the Cape Lopez Canyon, which incises the shelf to the edge of
682   the Mandji Island (Biscara et al., 2013). The deep incision of the continental shelf up to
683   the coast combined with the longshore sediment transport along the Mandji Island and
684   the narrow shelf in this area (4 km wide) favor the capture of sediment by this canyon
685   during time of high sea-level (Reyre, 1984; Biscara et al., 2013). The northern lobe,
686   which is directly connected to the Cape Lopez lobe by Channel A, appears to be also
687   fed by terrigenous sediments during the Holocene. Core KC21, located at the entrance
688   of the northern lobe, is entirely composed of *facies 3*, even for sediments deposited
689   during MIS1 (Figure 5).
690   In the Ogooue Fan, the shelf width between the littoral area and the canyon heads is the
691   main control factor on the fan activity. During periods of ~~relative~~ low sea-level, the
692   canyons of the central part of the system receive sediment from the river system that
693   extended across the subaerially exposed continental shelf. During periods of ~~relative~~
694   high sea-level, river sediments are unable to reach the canyon heads south of the Manji
695   Island and accumulate on the continental shelf close to the Ogooue Delta. However, part
696   of these sediments mixed with sediments coming from the south Gabon margin are drift-
697   transported and contribute to supply the Cape Lopez Canyon and consequently the Cape
698   Lopez and Northern Lobe. Due to their specific location and favorable hydrodynamic
699   conditions on the shelf, sedimentation on the Cape Lopez and the Northern lobes is
700   active during relative sea-level highstands, in contrast to the rest of the Ogooue Fan.
701   Examples of this type of supply have already been described along the California margin
702   where the La Jolla canyon is fed by drift-transported sediments during highstand
703   (Covault et al., 2007, 2011) but also on the southeast Australian coast near the Fraser
704   Island (Boyd et al., 2008), which appears very similar to the Mandji Island.

6   Conclusions

This study provides the first data on the morphology of the recent Ogooue Deep-sea fan and interpretations on sedimentary processes occurring in this environment. The Gabonese margin presents a pelagic/hemipelagic background sedimentation overprinted by downslope gravity flows. The fan is made up of various architectural elements and consists of both constructional and erosional sections. The pattern of sedimentation on the margin is controlled by subtle slope gradient changes ($< 0.3°$). The long-term interaction between gravity flows and the seafloor topography has induced the construction of successive depocenters and sediment bypass areas. The gravity flows have modified the topography according to a theoretical equilibrium profile, eroding the seafloor where slopes are steeper than the theoretical equilibrium profiles and depositing sediments when slopes are gentler than the theoretical equilibrium profile. Three successive main sediment depocenters have been identified along a longitudinal profile. They are associated with three areas of low slope gradient ($0.3°$-$0.2°$). The two updip deposition areas – the intermediate depocenter and the upper lobe area – have recorded coarse-grained sedimentation and are connected by a well-developed large mid-system valley measuring 100 km long and located on a steeper slope segment ($0.6°$). The distalmost depocenter – the lower lobe area - receive only the fine-grained portion of the sediment load that has bypassed the more proximal deposit areas. Sedimentation on this margin is made more complex by the presence of several volcanic islands and seamounts that constrain the gravity flows. The presence on the slope of the Mount Loiret has caused the formation of an isolated system composed of the Cape Lopez Canyon and lobe, which continues downstream by the Northern Lobe area. The Ogooue Fan is currently in a low activity period since the recent Holocene rise of sea-level. Nowadays, the sedimentation is mostly located on the shelf, in the Ogooue Delta and on the upper slope. The fan was more active during the last glacial lowstand. Nonetheless, the northern part of the system appears to have an asynchronous activity with the rest of the fan as this part is fed by the drift-transported sediments during time of relative high sea-level when the activity in the rest of the system is shut-down.

7 Acknowledgments

We thank the SHOM (hydrological and oceanographic marine service) for the data, the 'ARTEMIS' technical platform for radiocarbon age dating. We are also grateful to EPOC technicians and engineers: I. Billy, P. Lebleu, O. Ther and L. Rossignol for the data acquisition. P. Haugton and D.M. Hodgson are thanked for their constructive and helpful reviews.

8 References

Amy, L.A., Kneller, B.C., McCaffrey, W.D.: Facies architecture of the Grès de Peïra Cava, SE France: landward stacking patterns in ponded turbiditic basins. J. Geol. Soc. 164, 143–162. https://doi.org/10.1144/0016-76492005-019, 2007.

Anka, Z., Séranne, M., Lopez, M., Scheck-Wenderoth, M., Savoye, B.: The long-term evolution of the Congo deep-sea fan: A basin-wide view of the interaction between a giant submarine fan and a mature passive margin (ZaiAngo project). Tectonophysics 470, 42–56. https://doi.org/10.1016/j.tecto.2008.04.009, 2009.

Babonneau, N., Savoye, B., Cremer, M., Klein, B.: Morphology and architecture of the present canyon and channel system of the Zaire deep-sea fan. Mar. Pet. Geol. 19, 445–467. https://doi.org/10.1016/S0264-8172(02)00009-0, 2002.

Barfod, D.N., Fitton, J.G.: Pleistocene volcanism on São Tomé, Gulf of Guinea, West Africa. Quat. Geochronol. 21, 77–89. https://doi.org/10.1016/j.quageo.2012.11.006, 2014.

Beaubouef, R.T., Friedmann, S.J.: High resolution seismic/sequence stratigraphic framework for the evolution of Pleistocene intra slope basins, western Gulf of Mexico: depositional models and reservoir analogs., in: Deepwater Reservoirs of the World. Presented at the SEPM, 20th Annual Research Conference, pp. 40–60, 2000.

Bertoni, C., Cartwright, J.: 3D seismic analysis of slope-confined canyons from the Plio-Pleistocene of the Ebro Continental Margin (Western Mediterranean). Basin Res. 17, 43–62. https://doi.org/10.1111/j.1365-2117.2005.00254.x, 2005.

Biscara, L., Mulder, T., Hanquiez, V., Marieu, V., Crespin, J.-P., Braccini, E., Garlan, T.: Morphological evolution of Cap Lopez Canyon (Gabon): Illustration of lateral migration processes of a submarine canyon. Mar. Geol. 340, 49–56. https://doi.org/10.1016/j.margeo.2013.04.014, 2013.

Biscara, L., Mulder, T., Martinez, P., Baudin, F., Etcheber, H., Jouanneau, J.-M., Garlan, T.: Transport of terrestrial organic matter in the Ogooué deep sea turbidite system (Gabon). Mar. Pet. Geol. 28, 1061–1072. https://doi.org/10.1016/j.marpetgeo.2010.12.002, 2011.

Bouma, A.H., Coleman, J.M., Stelting, C.E., Kohl, B.: Influence of relative sea level changes on the construction of the Mississippi Fan. Geo-Mar. Lett. 9, 161–170. https://doi.org/10.1007/BF02431043, 1989.

Bouma, A.H., Treadwell, T.K.: Deep-sea dune-like features. Mar. Geol. 19, M53–M59. https://doi.org/10.1016/0025-3227(75)90078-X, 1975.

Bourget, J., Zaragosi, S., Ellouz-Zimmermann, S., Ducassou, E., Prins, M.A., Garlan, T., Lanfumey, V., Schneider, J.-L., Rouillard, P., Giraudeau, J.: Highstand vs. lowstand turbidite system growth in the Makran active margin: Imprints of high-frequency external controls on sediment delivery mechanisms to deep water systems. Mar. Geol. 274, 187–208. https://doi.org/10.1016/j.margeo.2010.04.005, 2010.

Bourget, J., Zaragosi, S., Garlan, T., Gabelotaud, I., Guyomard, P., Dennielou, B., Ellouz-Zimmermann, N., Schneider, J.: Discovery of a giant deep-sea valley in the Indian Ocean, off eastern Africa: The Tanzania channel. Mar. Geol. 255, 179–185. https://doi.org/10.1016/j.margeo.2008.09.002, 2008.

Bourgoin, J., Reyre, D., Magloire, P., Krichewsky, M.: Les canyons sous-marins du cap Lopez (Gabon). Cah Ocean. 6, 372–387, 1963.

Boyd, R., Ruming, K., Goodwin, I., Sandstrom, M., Schröder-Adams, C.: Highstand transport of coastal sand to the deep ocean: A case study from Fraser Island, southeast Australia. Geology 36, 15. https://doi.org/10.1130/G24211A.1, 2008.

Brooks, H.L., Hodgson, D.M., Brunt, R.L., Peakall, J., Poyatos-Moré, M., Flint, S.S.: Disconnected submarine lobes as a record of stepped slope evolution over multiple sea-level cycles. Geosphere 14, 1753–1779. https://doi.org/10.1130/GES01618.1, 2018.

Cameron, N.R., White, K.: Exploration Opportunities in Offshore Deepwater Africa. IBC 'Oil Gas Dev. West Afr. Lond. UK, 1999.

Chen, J.-C., Lo, C.Y., Lee, Y.T., Huang, S.W., Chou, P.C., Yu, H.S., Yang, T.F., Wang, Y.S., Chung, S.H.: Mineralogy and chemistry of cored sediments from active margin off southwestern Taiwan. Geochem. J. 41, 303–321, 2007.

Cita, M.B., Beghi, C., Camerlenghi, A., Kastens, K.A., McCoy, F.W., Nosetto, A., Parisi, E., Scolari, F., Tomadin, L.: Turbidites and megaturbidites from the Herodotus abyssal plain (eastern Mediterranean) unrelated to seismic events. Mar. Geol. 55, 79–101. https://doi.org/10.1016/0025-3227(84)90134-8, 1984.

Clift, P., Gaedicke, C.: Accelerated mass flux to the Arabian Sea during the middle to late Miocene. Geology 30, 207. https://doi.org/10.1130/0091-7613(2002)030<0207:AMFTTA>2.0.CO;2, 2002.

Covault, J.A., Normark, W.R., Romans, B.W., Graham, S.A.: Highstand fans in the California borderland: The overlooked deep-water depositional systems. Geology 35, 783. https://doi.org/10.1130/G23800A.1, 2007

Covault, J.A., Romans, B.W., Fildani, A., McGann, M., Graham, S.A.: Rapid Climatic Signal Propagation from Source to Sink in a Southern California Sediment-Routing System. J. Geol. 118, 247–259. https://doi.org/10.1086/651539, 2010.

Covault, J.A., Romans, B.W., Graham, S.A., Fildani, A., Hilley, G.E.: Terrestrial source to deep-sea sink sediment budgets at high and low sea levels: Insights from tectonically active Southern California. Geology 39, 619–622. https://doi.org/10.1130/G31801.1, 2011.

Damuth, J.: The Amazon-HARP Fan Model: Facies Distributions in Mud-Rich Deep-Sea Fans Based on Systematic Coring of Architectural Elements of Amazon Fan, 1995.

Damuth, J.E.: Neogene gravity tectonics and depositional processes on the deep Niger Delta continental margin. Mar. Pet. Geol. 11, 320–346. https://doi.org/10.1016/0264-8172(94)90053-1, 1994.

Damuth, J.E.: Use of high-frequency (3.5–12 kHz) echograms in the study of near-bottom sedimentation processes in the deep-sea: a review. Mar. Geol. 38, 51–75, 1980a.

Damuth, J.E.: Quaternary sedimentation processes in the South China Basin as revealed by echo-character mapping and piston-core studies, in: Hayes, D.E. (Ed.), Geophysical Monograph Series. American Geophysical Union, Washington, D. C., pp. 105–125. https://doi.org/10.1029/GM023p0105, 1980b.

Damuth, J.E.: Echo character of the western equatorial Atlantic floor and its relationship to the dispersal and distribution of terrigenous sediments. Mar. Geol. 18, 17–45. https://doi.org/10.1016/0025-3227(75)90047-X, 1975.

Damuth, J.E., Embley, R.W.: Upslope flow of turbidity currents on the northwest flank of the Ceara Rise: western Equatorial Atlantic*. Sedimentology 26, 825–834. https://doi.org/10.1111/j.1365-3091.1979.tb00975.x, 1979.

Damuth, J.E., Hayes, D.E.: Echo character of the East Brazilian continental margin and its relationship to sedimentary processes. Mar. Geol. 24, 73–95. https://doi.org/10.1016/0025-3227(77)90002-0, 1977.

Demyttenaere, R., Tromp, J.P., Ibrahim, A., Allman-Ward, P.: Brunei Deep Water Exploration: From Sea Floor Images and Shallow Seismic Analogues to Depositional Models in a Slope Turbidite Setting, in: Weimer, P. (Ed.), Deep-Water Reservoirs of the World: 20th Annual. Society of economic palaeontologists and mineralogists, pp. 304–317. https://doi.org/10.5724/gcs.00.20, 2000.

Deptuck, M.E.: Pleistocene Seascape Evolution Above A "Simple" Stepped Slope—Western Niger Delta, in: Prather, B.E., Deptuck, M.E., Mohrig, D., Van Hoorn, B., Wynn, R.B. (Eds.), Application of the Principles of Seismic Geomorphology to Continental-Slope and Base-of-Slope Systems: Case Studies from Seafloor and Near-Seafloor Analogues. SEPM (Society for Sedimentary Geology). https://doi.org/10.2110/pec.12.99, 2012.

Deptuck, M.E., Steffens, G.S., Barton, M., Pirmez, C.: Architecture and evolution of upper fan channel-belts on the Niger Delta slope and in the Arabian Sea. Mar. Pet. Geol. 20, 649–676. https://doi.org/10.1016/j.marpetgeo.2003.01.004, 2003.

Deptuck, M.E., Sylvester, Z., Pirmez, C., O'Byrne, C.: Migration–aggradation history and 3-D seismic geomorphology of submarine channels in the Pleistocene Benin-

major Canyon, western Niger Delta slope. Mar. Pet. Geol. 24, 406–433. https://doi.org/10.1016/j.marpetgeo.2007.01.005, 2007.

Déruelle, B., Ngounouno, I., Demaiffe, D.: The 'Cameroon Hot Line' (CHL): A unique example of active alkaline intraplate structure in both oceanic and continental lithospheres. Comptes Rendus Geosci. 339, 589–600. https://doi.org/10.1016/j.crte.2007.07.007, 2007.

Dill, R.F., Dietz, R.S., Stewart, H.: deep-sea channels and delta of the Monterey submarine canyon. Geol. Soc. Am. Bull. 65, 191. https://doi.org/10.1130/0016-7606(1954)65[191:DCADOT]2.0.CO;2, 1954.

Droz, L., Marsset, T., Ondras, H., Lopez, M., Savoye, B., Spy-Anderson, F.-L.: Architecture of an active mud-rich turbidite system: The Zaire Fan (Congo–Angola margin southeast Atlantic): Results from ZaAngo 1 and 2 cruises. AAPG Bull. 87, 1145–1168, 2003.

Droz, L., Rigaut, F., Cochonat, P., Tofani, R.: Morphology and recent evolution of the Zaire turbidite system (Gulf of Guinea). Geol. Soc. Am. Bull. 108, 253–269. https://doi.org/10.1130/0016-7606(1996)108<0253:MAREOT>2.3.CO;2, 1996.

Embley, R.W.: New evidence for occurrence of debris flow deposits in the deep sea. Geology 4, 371. https://doi.org/10.1130/0091-7613(1976)4<371:NEFOOD>2.0.CO;2, 1976.

Ferry, J.-N., Mulder, T., Parize, O., Raillard, S.: Concept of equilibrium profile in deep-water turbidite system: effects of local physiographic changes on the nature of sedimentary process and the geometries of deposits. Geol. Soc. Lond. Spec. Publ. 244, 181–193. https://doi.org/10.1144/GSL.SP.2005.244.01.11, 2005.

Field, M.E., Gardner, J.V.: Pliocene-Pleistocene growth of the Rio Ebro margin, northeast Spain: A prograding-slope model. Geol. Soc. Am. Bull. 102, 721–733. https://doi.org/10.1130/0016-7606(1990)102<0721:PPGOTR>2.3.CO;2, 1990.

Fildani, A., Normark, W.R.: Late Quaternary evolution of channel and lobe complexes of Monterey Fan. Mar. Geol. 206, 199–223. https://doi.org/10.1016/j.margeo.2004.03.001, 2004.

Flood, R.D., Piper, D.J.W.: Amazon Fan sedimentation: the relationship to equatorial climate change, continental denudation, and sea-level fluctuations., in: Flood, R.D., Piper, D.J.W., Klaus, A., Peterson, L.C. (Eds.), Proceeding of the Ocean Drilling Program, Scientific Results. pp. 653–675, 1997.

Garcia, M., Parker, G.: Experiments on hydraulic jumps in turbidity currents near a canyon-fan transition. Science 245, 393–396. https://doi.org/10.1126/science.245.4916.393, 1989.

Garlan, T., Biscara, L., Guyomard, P., Le Faou, Y., Gabelotaud, I.: Rapport de la campagne MOCOSED 2010, Modèle de couches sédimentaires du Golfe de Guinée (Rapport de mission). SHOM, 2010.

Gaullier, V., Bellaiche, G.: Near-bottom sedimentation processes revealed by echo-character mapping studies, north-western Mediterranean Basin. AAPG Bull. 82, 1140–1155, 1998.

897 Gay, A., Lopez, M., Cochonat, P., Sultan, N., Cauquil, E., Brigaud, F.: Sinuous
898   pockmark belt as indicator of a shallow buried turbiditic channel on the lower
899   slope of the Congo basin, West African margin. Geol. Soc. Lond. Spec. Publ.
900   216, 173–189. https://doi.org/10.1144/GSL.SP.2003.216.01.12, 2003.
901 Gee, M.J.R., Gawthorpe, R.L.: Submarine channels controlled by salt tectonics:
902   Examples from 3D seismic data offshore Angola. Mar. Pet. Geol. 23, 443–458.
903   https://doi.org/10.1016/j.marpetgeo.2006.01.002, 2006.
904 Gee, M.J.R., Gawthorpe, R.L., Bakke, K., Friedmann, S.J.: Seismic Geomorphology
905   and Evolution of Submarine Channels from the Angolan Continental Margin. J.
906   Sediment. Res. 77, 433–446. https://doi.org/10.2110/jsr.2007.042, 2007.
907 Giresse, P.: Carte sédimentologique des fonds sous-marins du delta de l'Ogooué, 1969.
908 Giresse, P., Odin, G.S.: Nature minéralogique et origine des glauconies du plateau
909   continental du Gabon et du Congo. Sedimentology 20, 457–488, 1973.
910 Guillou, R.: MOCOSED 2010 cruise, Pourquoi pas ?
911   https://doi.org/10.17600/10030110, 2010.
912 Hanquiez, V., Mulder, T., Lecroart, P., Gonthier, E., Marchès, E., Voisset, M.: High
913   resolution seafloor images in the Gulf of Cadiz, Iberian margin. Mar. Geol. 246,
914   42–59. https://doi.org/10.1016/j.margeo.2007.08.002, 2007.
915 Hay, D.: Stratigraphic evolution of a tortuous corridor from the stepped slope of Angola,
916   in: Prather, B.E., Deptuck, M.E., Mohrig, D., Van Hoorn, B., Wynn, R.B. (Eds.),
917   Application of the Principles of Seismic Geomorphology to Continental-Slope
918   and Base-of-Slope Systems: Case Studies from Seafloor and Near-Seafloor
919   Analogues. SEPM (Society for Sedimentary Geology).
920   https://doi.org/10.2110/pec.12.99, 2012.
921 Heezen, B.C., Tharp, M., Ewing, M.: The Floors of the Oceans, in: Geological Society
922   of America Special Papers. Geological Society of America, pp. 1–126.
923   https://doi.org/10.1130/SPE65-p1, 1959.
924 Jacobi, R.D.: Sediment slides on the northwestern continental margin of Africa. Mar.
925   Geol. 22, 157–173. https://doi.org/10.1016/0025-3227(76)90045-1, 1976.
926 Jansen, J.H.F., Van Weering, T.C.E., Gieles, R., Van Iperen, J.: Middle and late
927   Quaternary oceanography and climatology of the Zaire-Congo fan and the
928   adjacent eastern Angola Basin. Neth. J. Sea Res. 17, 201–249, 1984.
929 Jegou, I., Savoye, B., Pirmez, C., Droz, L.: Channel-mouth lobe complex of the recent
930   Amazon Fan: The missing piece. Mar. Geol. 252, 62–77.
931   https://doi.org/10.1016/j.margeo.2008.03.004, 2008.
932 Jobe, Z.R., Lowe, D.R., Uchytil, S.J.: Two fundamentally different types of submarine
933   canyons along the continental margin of Equatorial Guinea. Mar. Pet. Geol. 28,
934   843–860. https://doi.org/10.1016/j.marpetgeo.2010.07.012, 2011.
935 Jobe, Z.R., Sylvester, Z., Howes, N., Pirmez, C., Parker, A., Cantelli, A., Smith, R.,
936   Wolinsky, M.A., O'Byrne, C., Slowey, N., Prather, B.: High-resolution,
937   millennial-scale patterns of bed compensation on a sand-rich intraslope
938   submarine fan, western Niger Delta slope. Geol. Soc. Am. Bull. 129, 23–37.
939   https://doi.org/10.1130/B31440.1, 2017.

940   Kane, I.A., Catterall, V., McCaffrey, W.D., Martinsen, O.J.: Submarine channel
941   response to intrabasinal tectonics: The influence of lateral tilt. AAPG Bull. 94,
942   189–219. https://doi.org/10.1306/08180909059, 2010.
943   Kane, I.A., Hodgson, D.M.: Sedimentological criteria to differentiate submarine
944   channel levee subenvironments: Exhumed examples from the Rosario Fm.
945   (Upper Cretaceous) of Baja California, Mexico, and the Fort Brown Fm.
946   (Permian), Karoo Basin, S. Africa. Mar. Pet. Geol. 28, 807–823.
947   https://doi.org/10.1016/j.marpetgeo.2010.05.009, 2011.
948   Kenyon, N.H., Millington, J., Droz, L., Ivanov, M.K.: Scour holes in a channel-lobe
949   transition zone on the Rhône Cone, in: Atlas of Deep Water Environments.
950   Springer, Dordrecht, pp. 212–215. https://doi.org/10.1007/978-94-011-1234-
951   5_31, 1995.
952   Kneller, B.: Beyond the turbidite paradigm: physical models for deposition of turbidites
953   and their implications for reservoir prediction. Geol. Soc. Lond. Spec. Publ. 94,
954   31–49. https://doi.org/10.1144/GSL.SP.1995.094.01.04, 1995.
955   Kolla, V.: A review of sinuous channel avulsion patterns in some major deep-sea fans
956   and factors controlling them. Mar. Pet. Geol. 24, 450–469.
957   https://doi.org/10.1016/j.marpetgeo.2007.01.004, 2007.
958   Kolla, V., Coumes, F.: Morphology, Internal Structure, Seismic Stratigraphy, and
959   Sedimentation of Indus Fan. AAPG Bull. 71, 650–677, 1987.
960   Komar, P.D.: Hydraulic jumps in turbidity currents. Bull. Geol. Soc. Am. 82, 1477–
961   1488. https://doi.org/10.1130/0016-7606(1971)82[1477:HJITC]2.0.CO;2, 1971.
962   Lebigre, J.M.: Les mangroves des rias du littoral gabonais, essai de cartographie
963   typologique. Rev. Bois For. Trop., 1983.
964   Lee, D.-C., Halliday, A.N., Fitton, J.G., Poli, G.: Isotopic variations with distance and
965   time in the volcanic islands of the Cameroon line: evidence for a mantle plume
966   origin. Earth Planet. Sci. Lett. 123, 119–138. https://doi.org/10.1016/0012-
967   821X(94)90262-3, 1994.
968   Lerique, J., Barret, J., Walter, R.: Hydrographie, hydrologie, in: Géographie et
969   cartographie du Gabon : atlas illustré. EDICEF, Paris, pp. 14–17, 1983.
970   Lombo Tombo, S., Dennielou, B., Berné, S., Bassetti, M.-A., Toucanne, S., Jorry, S.J.,
971   Jouet, G., Fontanier, C.: Sea-level control on turbidite activity in the Rhone
972   canyon and the upper fan during the Last Glacial Maximum and Early deglacial.
973   Sediment. Geol. 323, 148–166. https://doi.org/10.1016/j.sedgeo.2015.04.009,
974   2015.
975   Loncke, L., Droz, L., Gaullier, V., Basile, C., Patriat, M., Roest, W.: Slope instabilities
976   from echo-character mapping along the French Guiana transform margin and
977   Demerara abyssal plain. Mar. Pet. Geol. 26, 711–723.
978   https://doi.org/10.1016/j.marpetgeo.2008.02.010, 2009.
979   Lonergan, L., Jamin, N.H., Jackson, C.A.-L., Johnson, H.D.: U-shaped slope gully
980   systems and sediment waves on the passive margin of Gabon (West Africa). Mar.
981   Geol. 337, 80–97. https://doi.org/10.1016/j.margeo.2013.02.001, 2013.

982 Mahé, G., Lerique, J., Olivry, J.-C.: Le fleuve Ogooué au Gabon : reconstitution des
983   débits manquants et mise en évidence de variations climatiques à l'équateur.
984   Hydrol Cont. 5, 105–124, 1990.
985 Masson, D.G.: Late Quaternary turbidity current pathways to the Madeira Abyssal Plain
986   and some constraints on turbidity current mechanisms. Basin Res. 6, 17–33.
987   https://doi.org/10.1111/j.1365-2117.1994.tb00072.x, 1994.
988 Masson, D.G., Kenyon, N.H., Gardner, J.V., Field, M.E.: Monterey Fan: channel and
989   overbank morphology, in: Pickering, K.T., Hiscott, R.N., Kenyon, N.H., Ricci
990   Lucchi, F., Smith, R.D.A. (Eds.), Atlas of Deep Water Environments. Springer
991   Netherlands, Dordrecht, pp. 74–79. https://doi.org/10.1007/978-94-011-1234-
992   5_13, 1995.
993 McGilvery, T.A., Cook, D.L.: The Influence of Local Gradients on Accommodation
994   Space and Linked Depositional Elements Across a Stepped Slope Profile,
995   Offshore Brunei, in: Roberts, H.R., Rosen, N.C., Fillon, R.F., Anderson, J.B.
996   (Eds.), Shelf Margin Deltas and Linked Down Slope Petroleum Systems: 23rd
997   Annual. SOCIETY OF ECONOMIC PALEONTOLOGISTS AND
998   MINERALOGISTS. https://doi.org/10.5724/gcs.03.23, 2003.
999 Menard, H.W.: Deep-Sea Channels, Topography, and Sedimentation. AAPG Bull. 39,
1000   255, 1955.
1001 Migeon, S., Weber, O., Faugeres, J.-C., Saint-Paul, J.: SCOPIX: A new X-ray imaging
1002   system for core analysis. Geo-Mar. Lett. 18, 251–255.
1003   https://doi.org/10.1007/s003670050076, 1998.
1004 Mignard, S.L.-A., Mulder, T., Martinez, P., Charlier, K., Rossignol, L., Garlan, T.:
1005   Deep-sea terrigenous organic carbon transfer and accumulation: Impact of sea-
1006   level variations and sedimentation processes off the Ogooue River (Gabon). Mar.
1007   Pet. Geol. 85, 35–53. https://doi.org/10.1016/j.marpetgeo.2017.04.009, 2017.
1008 Mougamba, R.: Chronologie et architechture des systems turbiditiquess Cénozoïques
1009   du Prisme sédimentaire de l'Ogooué (Marge Nord-Gabon). Université de Lille,
1010   Lille, 1999.
1011 Mouscardes, P.: OPTIC CONGO 2 cruise, RV Beautemps-Beaupré [www Document].
1012   URL http://campagnes.flotteoceanographique.fr/campagnes/5090050/fr/
1013   (accessed 7.5.18), 2005.
1014 Mulder, T., Alexander, J.: Abrupt change in slope causes variation in the deposit
1015   thickness of concentrated particle-driven density currents. Mar. Geol. 175, 221–
1016   235. https://doi.org/10.1016/S0025-3227(01)00114-1, 2001.
1017 Mulder, T., Etienne, S.: Lobes in deep-sea turbidite systems: State of the art. Sediment.
1018   Geol. 229, 75–80. https://doi.org/10.1016/j.sedgeo.2010.06.011, 2010.
1019 Normark, W.R., Barnes, N.E., Coumes, F.: Rhone Deep-Sea Fan: A review. Geo-Mar.
1020   Lett. 3, 155–160. https://doi.org/10.1007/BF02462461, 1983.
1021 Normark, W.R., Damuth, J.E.: Sedimentary facies and associated depositional elements
1022   of the Amazon Fan, Proceedings of the Ocean Drilling Program. Ocean Drilling
1023   Program. https://doi.org/10.2973/odp.proc.sr.155.1997, 1997.

Normark, W.R., Piper, D.J.W.: Initiation processes and flow evolution of turbidity currents: implications for the depositional record, in: From Shoreline to Abyss, SEPM Special Publication. pp. 207–230, 1991.

Normark, W.R., Posamentier, H., Mutti, E.: Turbidite systems: State of the art and future directions. Rev. Geophys. 31, 91–116. https://doi.org/10.1029/93RG02832, 1993.

O'Byrne, C., Prather, B., Pirmez, C., Steffens, G.S.: Reservoir architectural styles across stepped slope profiles: Implications for exploration, appraisal and development. Presented at the AAPG International conference, 2004.

Olausson, E.: Oxygen and carbon isotope analyses of a late quaternary core in the Zaire (Congo) fan. Neth. J. Sea Res. 17, 276–279. https://doi.org/10.1016/0077-7579(84)90050-4, 1984.

Peakall, J., McCaffrey, B., Kneller, B.: A Process Model for the Evolution, Morphology, and Architecture of Sinuous Submarine Channels. J. Sediment. Res. 70, 434–448. https://doi.org/10.1306/2DC4091C-0E47-11D7-8643000102C1865D, 2000.

Pettingill, H.S., Weimer, P.: Worlwide deepwater exploration and production: Past, present, and future. Lead. Edge 21, 371–376. https://doi.org/10.1190/1.1471600, 2002.

Pickering, K., Stow, D., Watson, M., Hiscott, R.: Deep-water facies, processes and models: a review and classification scheme for modern and ancient sediments. Earth Sci. Rev. 23, 75–174. https://doi.org/10.1016/0012-8252(86)90001-2, 1986.

Pilcher, R., Argent, J.: Mega-pockmarks and linear pockmark trains on the West African continental margin. Mar. Geol. 244, 15–32. https://doi.org/10.1016/j.margeo.2007.05.002, 2007.

Piper, D.J.W., Normark, W.R.: Processes That Initiate Turbidity Currents and Their Influence on Turbidites: A Marine Geology Perspective. J. Sediment. Res. 79, 347–362. https://doi.org/10.2110/jsr.2009.046, 2009.

Piper, D.J.W., Normark, W.R.: Sandy fans--from Amazon to Hueneme and beyond. AAPG Bull. 85, 1407–1438, 2001.

Pirmez, C., Beaubouef, R.T., Friedmann, S.J., Mohrig, D.C.: Equilibrium Profile and Baselevel in Submarine Channels: Examples from Late Pleistocene Systems and Implications for the Architecture of Deepwater Reservoirs, in: Weimer, P. (Ed.), Deep-Water Reservoirs of the World. https://doi.org/10.5724/gcs.00.20, 2000.

Prather, B.E.: Controls on reservoir distribution, architecture and stratigraphic trapping in slope settings. Mar. Pet. Geol. 20, 529–545. https://doi.org/10.1016/j.marpetgeo.2003.03.009, 2003.

Prather, B.E., Booth, J.R., Steffens, G.S., Craig, P.A.: Classification, Lithologic Calibration, and Stratigraphic Succession of Seismic Facies of Intraslope Basins, Deep-Water Gulf of Mexico. AAPG Bull. 82, 701–728, 1998.

Prather, B.E., O'Byrne, C., Pirmez, C., Sylvester, Z.: Sediment partitioning, continental slopes and base-of-slope systems. Basin Res. 29, 394–416. https://doi.org/10.1111/bre.12190, 2017.

1067 Pratson, L.F., Coakley, B.J.: A model for the headward erosion of submarine canyons
1068   induced by downslope-eroding sediment flows. Geol. Soc. Am. Bull. 108, 225–
1069   234. https://doi.org/10.1130/0016-7606(1996)108<0225:AMFTHE>2.3.CO;2,
1070   1996.
1071 Pratson, L.F., Laine, E.P.: The relative importance of gravity-induced versus current-
1072   controlled sedimentation during the Quaternary along the Mideast U.S. outer
1073   continental margin revealed by 3.5 kHz echo character. Mar. Geol. 89, 87–126.
1074   https://doi.org/10.1016/0025-3227(89)90029-7, 1989.
1075 Pratson, L.F., Ryan, W.B.F., Mountain, G.S., Twichell, D.C.: Submarine canyon
1076   initiation by downslope-eroding sediment flows: Evidence in late Cenozoic strata
1077   on the New Jersey continental slope. Geol. Soc. Am. Bull. 106, 395–412.
1078   https://doi.org/10.1130/0016-7606(1994)106<0395:SCIBDE>2.3.CO;2, 1994.
1079 Prélat, A., Hodgson, D.M.: The full range of turbidite bed thickness patterns in
1080   submarine lobes: controls and implications. J. Geol. Soc. 170, 209–214.
1081   https://doi.org/10.1144/jgs2012-056, 2013.
1082 Rasmussen, E.S.: Structural evolution and sequence formation offshore South Gabon
1083   during the Tertiary. Tectonophysics, Dynamics of Extensional Basins and
1084   Inversion Tectonics 266, 509–523. https://doi.org/10.1016/S0040-
1085   1951(96)00236-3, 1996.
1086 Reading, H.G., Richards, M.: Turbidite systems in deep-water basin margins classified
1087   by grain size and feeder system. AAPG Bull. 78, 792–822, 1994.
1088 Reimer, P.: IntCal13 and Marine13 Radiocarbon Age Calibration Curves 0–50,000
1089   Years cal BP. Radiocarbon 55, 1869–1887.
1090   https://doi.org/10.2458/azu_js_rc.55.16947, 2013.
1091 Reyre, D.: Evolution géologique et caractères pétroliers d'une marge passive: cas du
1092   bassin du Bas Congo–Gabon. Bull. Cent. Rech. Explor. Prod. Elf Aquitaine 8,
1093   303–332, 1984.
1094 Salles, L., Ford, M., Joseph, P.: Characteristics of axially-sourced turbidite
1095   sedimentation on an active wedge-top basin (Annot Sandstone, SE France). Mar.
1096   Pet. Geol. 56, 305–323. https://doi.org/10.1016/j.marpetgeo.2014.01.020, 2014.
1097 Séranne, M., Anka, Z.: South Atlantic continental margins of Africa: A comparison of
1098   the tectonic vs climate interplay on the evolution of equatorial West Africa and
1099   SW Africa margins. J. Afr. Earth Sci. 43, 283–300.
1100   https://doi.org/10.1016/j.jafrearsci.2005.07.010, 2005.
1101 Séranne, M., Bruguier, O., Moussavou, M.: U-Pb single zircon grain dating of Present
1102   fluvial and Cenozoic aeolian sediments from Gabon: consequences on sediment
1103   provenance, reworking, and erosion processes on the equatorial West African
1104   margin. Bull. Société Géologique Fr. 179, 29–40, 2008.
1105 Séranne, M., Nzé Abeigne, C.-R.: Oligocene to Holocene sediment drifts and bottom
1106   currents on the slope of Gabon continental margin (West Africa). Sediment. Geol.
1107   128, 179–199. https://doi.org/10.1016/S0037-0738(99)00069-X, 1999.

Shepard, F.P.: Submarine Canyons: Multiple Causes and Long-Time Persistence. AAPG Bull. 65. https://doi.org/10.1306/03B59459-16D1-11D7-8645000102C1865D, 1981.

Shepard, F.P.: submarine erosion, a discussion of recent papers. Geol. Soc. Am. Bull. 62, 1413. https://doi.org/10.1130/0016-7606(1951)62[1413:SEADOR]2.0.CO;2, 1951.

Shepard, F.P., Emery, K.O.: Submarine Topography off the California Coast: Canyons and Tectonic Interpretation, Geological Society of America Special Papers. Geological Society of America. https://doi.org/10.1130/SPE31, 1941.

Smith, R.: Silled sub-basins to connected tortuous corridors: sediment distribution systems on topographically complex sub-aqueous slopes. Geol. Soc. Lond. Spec. Publ. 222, 23–43. https://doi.org/10.1144/GSL.SP.2004.222.01.03, 2004.

Spychala, Y.T., Hodgson, D.M., Flint, S.S., Mountney, N.P.: Constraining the sedimentology and stratigraphy of submarine intraslope lobe deposits using exhumed examples from the Karoo Basin, South Africa. Sediment. Geol. 322, 67–81. https://doi.org/10.1016/j.sedgeo.2015.03.013, 2015.

Stanley, D.J., Moore, G.T.: The Shelfbreak: Critical Interface on Continental Margins. SEPM (Society for Sedimentary Geology). https://doi.org/10.2110/pec.83.33, 1983.

Stevenson, C.J., Jackson, C.A.-L., Hodgson, D.M., Hubbard, S.M., Eggenhuisen, J.T.: Deep-Water Sediment Bypass. J. Sediment. Res. 85, 1058–1081. https://doi.org/10.2110/jsr.2015.63, 2015.

Stevenson, C.J., Talling, P.J., Wynn, R.B., Masson, D.G., Hunt, J.E., Frenz, M., Akhmetzhanhov, A., Cronin, B.T.: The flows that left no trace: Very large-volume turbidity currents that bypassed sediment through submarine channels without eroding the sea floor. Mar. Pet. Geol. 41, 186–205. https://doi.org/10.1016/j.marpetgeo.2012.02.008, 2013.

Stow, D.A.V., Piper, D.J.W.: Deep-water fine-grained sediments: facies models. Geol. Soc. Lond. Spec. Publ. 15, 611–646. https://doi.org/10.1144/GSL.SP.1984.015.01.38, 1984.

Sylvester, Z., Cantelli, A., Pirmez, C.: Stratigraphic evolution of intraslope minibasins: Insights from surface-based model. AAPG Bull. 99, 1099–1129. https://doi.org/10.1306/01081514082, 2015.

Syvitski, J.P.M., Vörösmarty, C.J., Kettner, A.J., Green, P.: Impact of Humans on the Flux of Terrestrial Sediment to the Global Coastal Ocean. Science 308, 376–380. https://doi.org/10.1126/science.1109454, 2005.

Thornton, S.E.: Hemipelagites and Associated Facies of Slopes and Slope Basins. Geol. Soc. Lond. Spec. Publ. 15, 377–394, 1984.

Tripsanas, E.K., Phaneuf, B.A., Bryant, W.R.: Slope Instability Processes in a Complex Deepwater Environment, Bryant Canyon Area, Northwest Gulf of Mexico, in: Offshore Technology Conference. Presented at the Offshore Technology Conference, Offshore Technology Conference, Houston, Texas. https://doi.org/10.4043/14273-MS, 2002.

Twichell, D.C., Roberts, D.G.: Morphology, distribution, and development of submarine canyons on the United States Atlantic continental slope between Hudson arid Baltimore Canyons. Geology 10, 408. https://doi.org/10.1130/0091-7613(1982)10<408:MDADOS>2.0.CO;2, 1982.

Unterseh, S.: Cartographie et caractérisation du fond marin par sondeur multifaisceaux. Vandoeuvre-les-Nancy, INPL, 1999.

Van der Merwe, W.C., Hodgson, D.M., Brunt, R.L., Flint, S.S.: Depositional architecture of sand-attached and sand-detached channel-lobe transition zones on an exhumed stepped slope mapped over a 2500 km2 area. Geosphere 10, 1076–1093. https://doi.org/10.1130/GES01035.1, 2014.

Viana, A.R., Faugères, J.-C.: Upper slope sand deposits: the example of Campos Basin, a latest Pleistocene-Holocene record of the interaction between alongslope and downslope currents. Geol. Soc. Spec. Publ. 129, 287–316. https://doi.org/10.1144/GSL.SP.1998.129.01.18, 1998.

Volat, J.-L., Pastouret, L., Vergnaud-Grazzini, C.: Dissolution and carbonate fluctuations in Pleistocene deep-sea cores: A review. Mar. Geol. 34, 1–28. https://doi.org/10.1016/0025-3227(80)90138-3, 1980.

Weaver, P.P.E., Wynn, R.B., Kenyon, N.H., Evans, J.: Continental margin sedimentation, with special reference to the north-east Atlantic margin: Continental slope sedimentation. Sedimentology 47, 239–256. https://doi.org/10.1046/j.1365-3091.2000.0470s1239.x, 2000.

Wonham, J., Jayr, S., Mougamba, R., Chuilon, P.: 3D sedimentary evolution of a canyon fill (Lower Miocene-age) from the Mandorove Formation, offshore Gabon. Mar. Pet. Geol. 17, 175–197. https://doi.org/10.1016/S0264-8172(99)00033-1, 2000.

Wynn, R. B., Talling, P.J., Masson, D.G., Le Bas, T.P., Cronin, B.T., Stevenson, C.J.: The Influence of Subtle Gradient Changes on Deep-Water Gravity Flows: A Case Study From the Moroccan Turbidite System, in: Prather, B.E., Deptuck, M.E., Mohrig, D., Van Hoorn, B., Wynn, Russell B. (Eds.), Application of the Principles of Seismic Geomorphology to Continental-Slope and Base-of-Slope Systems: Case Studies from Seafloor and Near-Seafloor Analogues. SEPM (Society for Sedimentary Geology). https://doi.org/10.2110/pec.12.99, 2012.

Wynn, R.B., Cronin, B.T., Peakall, J.: Sinuous deep-water channels: Genesis, geometry and architecture. Mar. Pet. Geol. 24, 341–387. https://doi.org/10.1016/j.marpetgeo.2007.06.001, 2007.

Wynn, R.B., Masson, D.G., Stow, D.A., Weaver, P.P.: Turbidity current sediment waves on the submarine slopes of the western Canary Islands. Mar. Geol. 163, 185–198, 2000.

Wynn, R.B., Weaver, P.P.E., Masson, D.G., Stow, D.A.V.: Turbidite depositional architecture across three interconnected deep-water basins on the north-west African margin. Sedimentology 49, 669–695. https://doi.org/10.1046/j.1365-3091.2002.00471.x, 2002.

Zachariasse, W.J., Schmidt, R.R., Van Leeuwen, R.J.W.: Distribution of foraminifera and calcareaous nannoplankton in quaternary sediments of the eastern Angola

1194   basin in response to climatic and oceanic fluctuations. Neth. J. Sea Res. 17, 250–
1195   275, 1984.

1196

1197